Annu. Rev. Fluid Mech. 1998. 30:539–78
Copyright © 1998 by Annual Reviews Inc. All rights reserved

DIRECT NUMERICAL SIMULATION: A Tool in Turbulence Research

Parviz Moin and Krishnan Mahesh
Center for Turbulence Research, Stanford University, Stanford, CA 94305 and NASA Ames Research Center, Moffett Field, California 94035;
e-mail: moin@ctr-next12.stanford.edu; e-mail: krishnan@leland.stanford.edu

KEY WORDS: computational fluid dynamics, numerical resolution, hot-wire anemometry, vorticity, shock waves, turbulence modeling, boundary layer structure

ABSTRACT

We review the direct numerical simulation (DNS) of turbulent flows. We stress that DNS is a research tool, and not a brute-force solution to the Navier-Stokes equations for engineering problems. The wide range of scales in turbulent flows requires that care be taken in their numerical solution. We discuss related numerical issues such as boundary conditions and spatial and temporal discretization. Significant insight into turbulence physics has been gained from DNS of certain idealized flows that cannot be easily attained in the laboratory. We discuss some examples. Further, we illustrate the complementary nature of experiments and computations in turbulence research. Examples are provided where DNS data has been used to evaluate measurement accuracy. Finally, we consider how DNS has impacted turbulence modeling and provided further insight into the structure of turbulent boundary layers.

1. INTRODUCTION

Turbulence has been the victim of many colorful descriptions over the years, from Lamb's (1916) scholarly "chief outstanding difficulty of our subject" to Bradshaw's (1994) inspired "invention of the Devil on the seventh day of creation." This apparent frustration results largely from the mixture of chaos and order and the wide range of length and time scales that turbulent flows possess. The complex behavior of turbulence is the consequence of a fairly simple set of equations—the Navier-Stokes equations. However, analytical solutions to even the simplest turbulent flows do not exist. A complete description of a

0066-4189/98/0115-0539$08.00

turbulent flow, where the flow variables (e.g. velocity and pressure) are known as a function of space and time can therefore only be obtained by numerically solving the Navier-Stokes equations. These numerical solutions are termed direct numerical simulations (DNS in short), and are the subject of this paper.

The instantaneous range of scales in turbulent flows increases rapidly with the Reynolds number. As a result, most engineering problems, e.g. the flow around a car, have too wide a range of scales to be directly computed using DNS. The engineering computation of turbulent flows therefore relies on simpler descriptions: Instead of solving for the instantaneous flow-field, the *statistical* evolution of the flow is sought. Approaches based on the Reynolds-averaged Navier-Stokes (RANS) equations are the most prevalent (see Speziale 1991 for a review) and involve computing one-point moments such as mean velocity and turbulent kinetic energy. Another approximation, large eddy simulation (LES), is intermediate in complexity between DNS and RANS. Large eddy simulation directly computes the large energy-containing scales, while modeling the influence of the small scales (see Lesieur & Métais 1996, and Moin 1997 for a review).

Statistical descriptions suffer from the curse of closure, i.e. the equations describing the statistical evolution of the flow contain terms that cannot be obtained from the Navier-Stokes equations and therefore require modeling. As the complexity of the computed flows increases, improvement in the turbulence models is often sought. This search for better turbulence models, and better parameterization of the turbulence, is what drives most turbulence research. DNS is a tool in this endeavor, in which it complements the time-trusted methodology of experimental research.

The capabilities of this relatively new tool are impressive, and this article reviews its contributions to turbulence research. However, the fraternity of turbulence researchers is large and the areas of interest are diverse. In the interest of brevity, this review is restricted to the DNS of three-dimensional, fully turbulent, nonreacting, nongeophysical flows. Both incompressible and compressible flows are discussed. Transitional flows constitute an important application of DNS; however, the review by Kleiser & Zang (1991) allows their omission from this article. Computation of reacting flows is discussed by Poinsot & Vervisch elsewhere in this volume. The reader interested in the Reynolds stress modeling of turbulence will find the reviews by Reynolds (1976) and Speziale (1991) useful, while the theory and application of LES may be found in Lesieur & Métais (1996) and Moin (1997).

This paper is organized as follows. We provide a brief history of DNS in section 1.1. We emphasize the changes that have occurred since the review article by Rogallo & Moin (1984). The broadband nature of turbulence requires care to be taken in its numerical computation; section 2 therefore discusses some of the issues involved. Significant insight into turbulence physics has

been gained from DNS of certain idealized flows that cannot be easily attained in the laboratory. These studies, termed novel numerical experiments, are discussed in section 3. Section 4 then presents some examples that illustrate how experiments and computations can complement each other. The impact of DNS on turbulence modeling is discussed in section 5, followed in section 6 by the study of boundary layer structure using DNS. We conclude the paper in section 7.

1.1 *Background*

The foundations of DNS were laid at the National Center for Atmospheric Research (see Fox & Lilly 1972 for a review). The beginnings were humble: Orszag & Patterson (1972) performed a 32^3 computation of isotropic turbulence at a Reynolds number (based on Taylor microscale) of 35. Although the resolution used appears inadequate by today's standards, the calculations demonstrated how spectral methods could actually be used to perform large-scale computations of three-dimensional turbulence. The next major step was taken by Rogallo (1981), who combined a transformation of the governing equations with an extension of the Orszag-Patterson algorithm to compute homogeneous turbulence subjected to mean strain. Rogallo's study examined the effects of mean shear, irrotational strain, and rotation on homogeneous turbulence. The results were compared to theory and experimental data and used to evaluate several turbulence models. Rogallo's pioneering work set the standard for DNS of homogeneous turbulence. Subsequent homogeneous DNS have essentially used his algorithm.

The earliest computed flows were inhomogeneous in only one direction. The computing resources in the late 1970s did not allow DNS of wall-bounded turbulence; however, coarse-grid computations of free-shear layers (e.g. Riley & Metcalfe 1980) could be performed. Wall-bounded flows could clearly not be ignored; LES was therefore used (e.g. Moin & Kim 1982) to compute the simplest such flow—the fully developed plane channel. The results were then used to study the physics of near-wall turbulence (see Rogallo & Moin 1984). Despite the good qualitative agreement of flow visualization results with experiment, there was some concern about drawing definitive conclusions from a simulation that contained ad hoc models. It was not until 1987 that DNS of the plane channel was performed (Kim et al 1987). Interestingly, the plane channel DNS was actually preceded by DNS of the flow in a curved channel by Moser & Moin (1987). The channel flow has proven to be an extremely useful framework for the study of wall-bounded turbulence. Subsequent studies have modified the channel configuration to examine the response of wall-bounded turbulence to factors such as rotation (Kristoffersson & Andersson 1993), mean three-dimensionality (Moin et al 1990), transpiration (Sumitani & Kasagi 1995),

transverse curvature (Neves & Moin 1994), heat transfer (Kasagi et al 1992), and riblets (Choi et al 1992). The next major step was taken by Spalart (1986, 1988), who developed an ingenious method to compute the turbulent flat-plate boundary layer under zero and favorable pressure gradients. Spalart's boundary layer data have been widely used by workers in the field.

The computations outlined above were all homogeneous in the streamwise direction (in the coordinate system of solution); periodic boundary conditions were therefore imposed along that direction. Computing flows that are inhomogeneous in the streamwise direction requires turbulence to be specified at the inflow plane. A recent advance has been the development of methods to specify this inflow turbulence. As a result, reasonably complex flows, e.g. the flow over a backstep (Le & Moin 1994), and flat plate boundary layer separation (Na & Moin 1996) have been computed.

In contrast to its incompressible counterpart, DNS of compressible turbulent flows is fairly recent. The early 1980s saw DNS of homogeneous compressible turbulence being initiated (Feiereisen et al 1981). However, it was not until a decade later that serious study of compressible homogeneous turbulence (isotropic and sheared) was undertaken (Erlebacher et al 1990, Blaisdell et al 1993, Lee et al 1991, Sarkar et al 1991). Wall-bounded flows such as the compressible channel (Coleman et al 1995) and turbulent boundary layer (Rai et al 1995) have only recently been attempted. High-speed turbulent mixing layers have been the focus of much experimental attention; DNS of this flow was recently performed by Vreman et al (1996). Shock waves feature prominently in compressible flows; recent DNS (Lee et al 1993, Mahesh et al 1997) has examined their interaction with turbulence. An exciting new development has been the field of computational aeroacoustics, where both the fluid motion and the sound it radiates are directly computed (see Tam 1995, Lele 1997 for reviews). Computational aeroacoustics is still in its infancy; the sound from a canonical flow such as a perfectly expanded supersonic jet has only just been computed (J Freund, SK Lele & P Moin, unpublished information). Figure 1 shows results for a Mach 1.9 jet from their massive computations using $640 \times 270 \times 128$ mesh points.

In tracing the evolution of DNS over the past decade, one observes that the complexity of the computed flows has noticeably increased, but that their Reynolds numbers are still low. Incompressible flows were the focus of attention a decade ago; compressible, even reacting, flows are being computed today. Another development has been the increased investigation of turbulence physics by computing idealized flows that cannot easily be produced in the laboratory. As the geometry of the flows has evolved, so have the numerical methods. Current computations typically use finite-difference schemes, or a combination of spectral and finite-difference schemes, in contrast to the fully

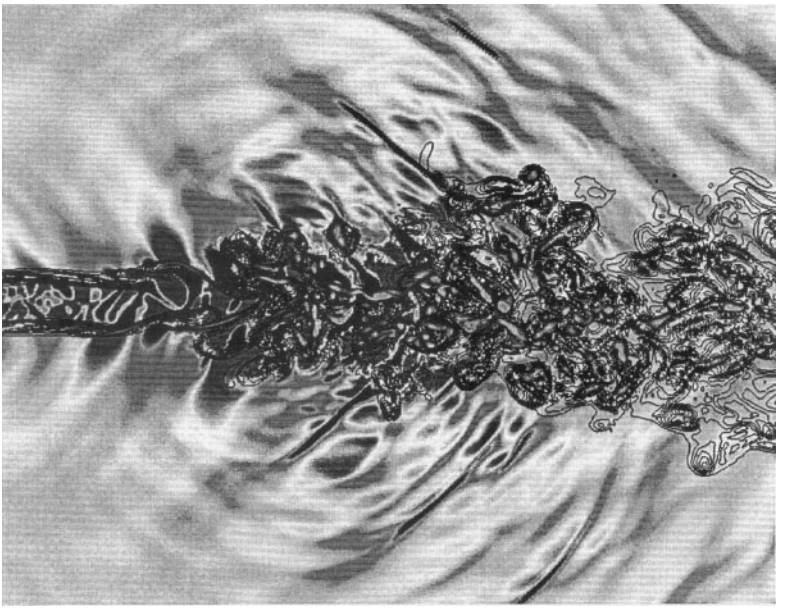

Figure 1 The sound radiated by a Mach 1.9 circular jet. Contours of vorticity (black) are overlaid on dilatation contours (gray). The computations were performed by J Freund, SK Lele & P Moin (unpublished information).

spectral algorithms used earlier. Finite element methods, and the use of unstructured grids are also being explored. These changes over the past decade have been accompanied by a significant improvement in computer hardware. A desktop computer like the 200 MHz Pentium Pro is about five times faster than the CDC7600 used by Orszag & Patterson in 1972 and the available memory is about two orders of magnitude greater. Currently available parallel machines like the 64 processor SP-2 are about 100 times faster than the 64 processor ILLIAC-IV used in the early 1980s.

2. NUMERICAL ISSUES

Numerical methods for the direct simulation of turbulence are required to accurately reproduce its evolution over a wide range of length and time scales. This section discusses some of the issues involved. Spatial discretization is considered in section 2.1. A discussion of time advancement in section 2.2 is followed in section 2.3 by an examination of the boundary conditions. Emphasis is placed on the specification of turbulence at inflow boundaries. Compressible turbulent

flows often interact with shock waves; section 2.4 considers their computation. Cost considerations restrict DNS to low Reynolds numbers; section 2.5 discusses this issue.

2.1 *Spatial Resolution*

The range of scales that need to be accurately represented in a computation is dictated by the physics. The grid determines the scales that are represented, while the accuracy with which these scales are represented is determined by the numerical method.

What are the largest and smallest scales that need to be resolved? Along statistically inhomogeneous directions, physical parameters such as channel width, boundary layer thickness, or mixing layer thickness determine the largest scales. Along homogeneous directions, where periodic boundary conditions are imposed, two-point correlations of the solution are required to decay nearly to zero within half the domain, to ensure proper statistical representation of the large scales. The Kolmogorov length scale, $\eta = (\nu^3/\epsilon)^{1/4}$, is commonly quoted as the smallest scale that needs to be resolved. However, this requirement is probably too stringent. The smallest resolved lengthscale is required to be of $O(\eta)$, not equal to η. Spectral DNS (listed in Table 1) shows very good agreement with experiments even though the Kolmogorov lengthscale is not resolved. Table 1 lists the resolution used in these computations. It appears that the relevant requirement to obtain reliable first and second order statistics is that the resolution be fine enough to accurately capture most of the dissipation. The smallest lengthscale that must be accurately resolved depends on the energy spectrum, and is typically greater than the Kolmogorov lengthscale; e.g. Moser & Moin (1987) note that most of the dissipation in the curved channel occurs at scales greater than 15η (based on average dissipation).

Table 1 Resolution (in Kolmogorov units) used in spectral simulations of some homogeneous and wall-bounded flows. η at the wall is used for the wall-bounded flows.[a]

Flow	Resolution in η
Curved channel (MM)	$\Delta z = 3.75$, $\Delta r = 0.13$, $r_c\,\Delta\theta = 11.25$
Plane channel (KMM)	$\Delta x = 7.5$, $\Delta y = 0.03$, $\Delta z = 4.4$
Boundary layer (S)	$\Delta x = 14.3$, $\Delta y = 0.33$, $\Delta z = 4.8$
Homogeneous shear (RMR)	$\Delta x = 7.8$, $\Delta y = 3.9$, $\Delta z = 3.9$
Isotropic turbulence (W)	$\Delta x = 4.5$, $\Delta y = 4.5$, $\Delta z = 4.5$

[a]MM, KMM, S, RMR, and W denote Moser & Moin 1987, Kim et al 1987, Spalart 1988 ($R_\theta = 1410$), Rogers et al 1986 (Run C128U), and Wray's (AA Wray, unpublished information) DNS of Comte-Bellot & Corrsin's (1971) experiment, respectively.

The resolution requirements are of course influenced by the numerical method used. Spectral methods were used by all the computations quoted in Table 1. Differencing schemes with larger numerical error would require higher resolution to achieve the same degree of accuracy. Spatial discretization error has two primary (coupled) components: differentiation error, and error associated with the nonlinearity of the governing equations. Fourier analysis, and the concept of the "modified wavenumber" is useful in quantifying the differentiation error. Consider a single Fourier mode in one dimension, namely $f = e^{ikx}$. Discretize f on a domain of length 2π, using a uniform mesh of N points. The mesh spacing $h = 2\pi/N$. The exact first derivative of f at the j^{th} node is ike^{ikx_j}; the numerically computed derivatives will be of the form $ik'e^{ikx_j}$. k' is a function of k and h, and is called the modified wavenumber for the first derivative operator; e.g. $k' = \sin kh/h$ for the second-order central difference scheme. The difference between k' and k provides the differentiation error as a function of the resolution of the wave.

The physics (e.g. dissipation spectrum) dictates the smallest wavenumber that needs to be resolved, and the accuracy with which it needs to be represented. Assume for example, that a wave with wavelength 3η is required to be differentiated with at least 5% accuracy. It is straightforward to show, using the modified wavenumber, that the second-order central difference requires a mesh spacing equal to 0.26η to meet this requirement, while the fourth-order central difference, sixth-order Padé, and Fourier spectral schemes require mesh spacings of 0.55η, 0.95η, and 1.5η respectively; i.e. the lower accuracy of the second order scheme translates into greater resolution requirements.

Differentiation error is only part of the error at small scales. There are two other sources of error that result from nonlinearity. The nonlinear terms in the equation produce a triadic interaction between the scales. The evolution of scales near the cut-off ($\lambda = 2h$) is therefore influenced by scales that are beyond the cut-off ($\lambda < 2h$), and are hence not represented by the grid. DNS requires that the resolution be fine enough for this error to be small. A more serious, and potentially catastrophic, source of error is aliasing. When functions are represented in terms of a finite number of basis functions (e.g. Fourier modes), nonlinear operations generate modes that are not in the set of modes being represented. A discrete representation mistakes these higher order modes for modes in the set. The contribution from these higher order modes is therefore improperly added to the modes in the set. This process is termed aliasing. The small scales have larger levels of aliasing error. Finite difference schemes typically have lower levels of aliasing error than spectral methods.

Aliasing error can cause either numerical instability or excessive turbulence decay. For example, Kim et al (1987) had to remove the aliasing errors (dealiasing) in order to compute the turbulent flow in a plane channel. The turbulence

was found to decay if dealiasing was not performed. Prior to this work, aliasing errors were thought to cause only numerical instability. As shown by Zang (1991), Kravchenko & Moin (1996), and Blaisdell et al (1996), the aliasing error in non-Galerkin formulations depends upon the analytical form of the nonlinear terms prior to discretization. When central differences are used, the skew-symmetric form of the nonlinear terms ($[u_j u_{i,j} + (u_i u_j)_{,j}]/2$), is seen to have lower levels of aliasing error for both incompressible and compressible DNS. The compressible equations contain division by density, and the viscosity-temperature relation, as two additional sources of aliasing. Lee et al (1992b) propose solving for the specific volume to avoid the aliasing resulting from division. With the exception of their work, little attention seems to have been devoted to these additional aliasing sources in the compressible equations.

For finite-difference schemes, the combination of higher levels of differentiation error and lower levels of nonlinear truncation and aliasing error determines the overall error at the small scales. This error, in conjunction with the spectrum of the solution, dictates the resolution requirements. A rule of thumb is that second-order central difference schemes require about twice the resolution (in each direction) to achieve the same results as a spectral DNS. Studies in plane channel flow (Choi et al 1992, Kristoffersen & Andersson 1993) show noticeable differences in the fluctuating shear stress, and higher-order quantities such as vorticity, between the second-order schemes and spectral methods. Turbulent kinetic energy profiles are seen to be less sensitive.

2.2 *Time Advancement*

A wide range of time scales puts turbulent flows into the category of stiff systems for time advancement. Stiff systems are routinely encountered in CFD calculations of steady aerodynamic flows, where they are handled using implicit time advancement algorithms and large time steps. It is tempting to adopt a similar practice in DNS. Unfortunately, the requirement of time accuracy over a wide range of scales does not permit very large timesteps in DNS. Use of large timesteps implies that the small scales can have large errors, which can corrupt the solution.

Von Neumann analysis may be used to illustrate the effect of time advancement on the error at different scales. Consider the one-dimensional advection equation ($f_t + c f_x = 0$) on a periodic domain. The solution may be represented as a summation of Fourier modes. Consider a single Fourier mode. Spatial differencing yields the ordinary differential equation, $d\widehat{f}/dt = -ik'\widehat{f}$, where k' denotes the modified wavenumber discussed in section 2.1. It is straightforward to obtain the (complex) amplification factor (ratio of the solution at consecutive timesteps), $\sigma = \widehat{f}_{n+1}/\widehat{f}_n$, when the above ODE is numerically integrated. The amplification factor thus obtained is a function of $k'h$ and the CFL number,

$c\Delta t/h$. The amplitude and phase errors introduced by the time-discretization may therefore be examined as a function of kh for different values of the CFL number. Note that the amplitude ratio of the exact solution is unity. Figure 2 examines the error in amplitude when a combination of the sixth-order Padé scheme and fourth-order Runge-Kutta scheme is used for spatial differencing and time advancement, respectively. The strong influence of timestep on the small scale error is apparent. Note also that the fully discretized equations now have a dissipative character, although the spatial discretization is nondissipative.

Does this imply that only explicit time advancement may be used for DNS? Not necessarily. The range of frequencies that need to be accurately represented is dictated by the physics. The grid, spatial differencing scheme, and the solution determine the range of frequencies represented by the discrete equations. Implicit time advancement becomes attractive when the discrete equations represent frequencies far higher than those required by the physics. A common practice in incompressible DNS of wall-bounded flows is to use implicit time advancement for the viscous terms and explicit time advancement

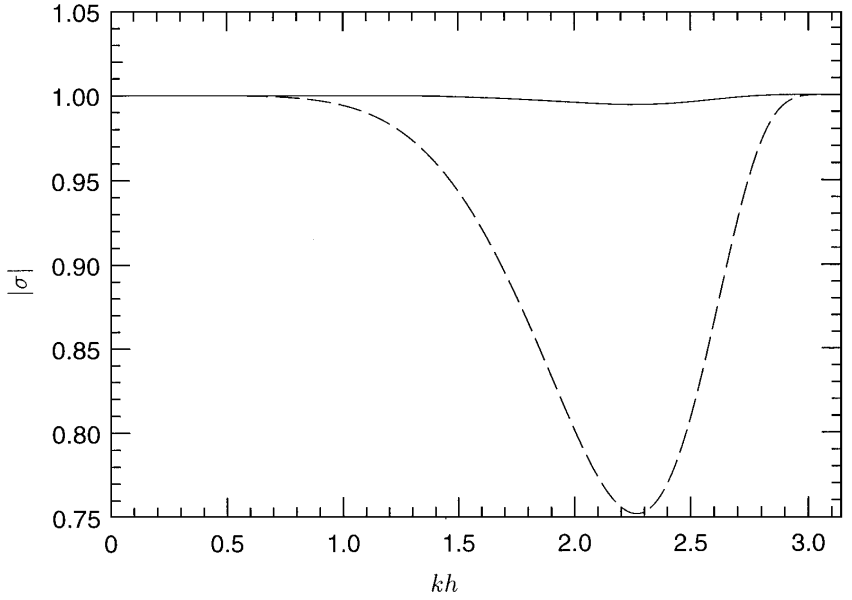

Figure 2 The influence of discrete time-advancement on small-scale accuracy. The amplitude ratio is plotted as a function of resolution. The sixth order Padé scheme is used for spatial differencing, while the fourth order Runge-Kutta scheme is used for time advancement. Solid CFL = 0.5, dashed CFL = 1. The stability limit is CFL = 1.43.

for the convection terms. Integrating factors may be used for the viscous term in homogeneous incompressible computations (Rogallo 1981). A general statement about the appropriateness of using implicit time advancement for the convection terms cannot be made. For example, Choi & Moin (1994) examined the possibility of using a fully implicit algorithm in turbulent channel flow. Very large timesteps were found to cause the turbulence in the channel to decay to a laminar state. At timesteps small enough for time accuracy to be maintained, the overhead associated with the implicit algorithm made it uncompetitive with explicit time advancement for the convection terms. However, in computations of the flow over riblets (Choi et al 1992), the grid clustering around the peaks of the riblets required a fully implicit algorithm for economical calculations.

2.3 *Boundary Conditions*

Specifying boundary conditions at open boundaries is a difficult issue in DNS. Given a turbulent flow, the only "correct" boundary condition at an arbitrary surface in the flow is the solution itself. But if the solution is already known, why compute the flow?

Consider incompressible flow. Statistically homogeneous directions such as the spanwise direction in a two-dimensional boundary layer are straightforward to treat—periodic conditions are imposed. Accurate and efficient ways of treating the far-field of vortically compact flows such as boundary layers, mixing layers, and wakes also exist (see e.g. Rogallo & Moin 1984, Spalart et al 1991, Corral & Jiménez 1995). The major difficulty is posed by the inflow and outflow boundary conditions. Fully developed flows such as the turbulent channel or pipe are homogeneous in the streamwise direction, but this is not the case for most flows. If complex flows are to be computed, turbulent inflow and outflow boundary conditions are required.

Early DNS circumvented this problem by appealing to Taylor's hypothesis. The turbulence was assumed to be homogeneous in the streamwise direction, as a result of which it evolved statistically in time (temporal simulations). A convection velocity was then used to relate the temporal evolution of the simulation to the spatial evolution seen in experiments. This approach works very well for a limited class of flows; examples include decaying grid turbulence, homogeneous shear flows, plane mixing layers, and turbulence passing through axisymmetric contractions and expansions. Note that the mean flow is constant in the streamwise direction in temporal simulations, i.e., the mean streamlines are parallel. Nonparallel effects that are present in the laboratory are therefore not represented. Spalart (1988) devised an ingenious coordinate transformation to overcome this limitation in DNS of the turbulent boundary layer. The transformation allowed periodic boundary conditions to be used in the streamwise

direction while generating a statistically stationary turbulent flow whose statistics corresponded to a single experimental streamwise station.

However, Spalart's approach is restricted to flows whose mean streamwise variation is small as compared to the transverse variation. DNS of more complex flows must specify turbulent inflow and outflow boundary conditions. The earliest methods for specification of inflow turbulence (Le & Moin 1994, Lee et al 1992a) essentially generated a three-dimensional, divergence-free field of random fluctuations that was homogeneous in the streamwise direction and had prescribed second order statistics. This field of turbulence was then convected through the inflow plane using Taylor's hypothesis. In addition, the disturbances were randomized in time to prevent them from being time-periodic. The inflow disturbances evolved into "realistic" turbulence after a fairly large distance [e.g. 50 displacement thicknesses in the inlet channel of Le & Moin's (1994) DNS of the backstep]. However, they did allow computations such as flow over a backstep, and isotropic turbulence/shock wave interaction to be performed for the first time. The method of generating inflow turbulence has improved since then. As opposed to convecting a field of random numbers, recent DNS (e.g. Na & Moin 1996, Akselvoll & Moin 1996, Mahesh et al 1997) have convected an instantaneous turbulent field obtained from a separate temporal simulation. The evolution distances are noticeably shorter; e.g. 20 displacement thicknesses in Na & Moin's computations. A wide range of flows have been computed using this approach. Work on the inflow specification is still in progress; e.g. Lund et al (1996) present a simplified version of Spalart's approach, which shows promise as an inflow turbulence generator.

Compressibility introduces additional boundary-condition issues. Characteristic analysis (see e.g. Poinsot & Lele 1992) must be used in compressible DNS to determine the number of boundary conditions required. Acoustic waves from the domain interior can influence the solution at the inflow plane. If this influence is not accounted for in the inflow specification, acoustic waves will reflect from the inflow boundary back into the solution domain. Moreover, the validity of Taylor's hypothesis is suspect for compressible flows. Because acoustic waves and the vortical field travel at different speeds in the linear limit, using a single convection velocity for the inflow turbulence is valid only for low levels of compressibility (turbulent Mach number, $M_t < 0.5$ for isotropic turbulence according to Lee et al 1992a). Fortunately, most compressible flows of current interest are well below this level of turbulent compressibility. The outflow boundary conditions in compressible DNS are similarly required to suppress nonphysical reflections/generation of acoustic waves at the outflow plane. Considerable work on nonreflecting boundary conditions has been performed by workers in aeroacoustics (see Lele 1997 for a review). Typically, formulations used in aeroacoustics are used by current compressible DNS.

2.4 *Shock Waves*

Shock waves in compressible turbulent flows pose severe challenges to DNS. Consider the interaction of isotropic turbulence with a normal shock wave. At low Reynolds numbers, the three-dimensional energy spectrum of the turbulence may be approximated by $E(k) \sim (k/k_0)^4 \, \mathrm{e}^{-2(k/k_0)^2}$, where k_0 denotes the wavenumber at which the spectrum peaks. Assuming that the change in the upstream Mach number caused by the turbulent fluctuations is small, the shock thickness may be approximated by its laminar value (Thompson 1984); i.e.

$$\frac{\overline{c}\delta}{\overline{v}} = \frac{6.89}{M-1}, \tag{1}$$

where δ, $\overline{c}$ and M denote the shock thickness, the mean upstream sound speed, and mean upstream Mach number, respectively. Denoting the Kolmogorov length scale of the upstream turbulence by η, it is straightforward to show that

$$\frac{\eta}{\delta} = 0.13 \frac{M-1}{M_t} \sqrt{R_\lambda}, \tag{2}$$

where $M_t = 3^{1/2} u_{\mathrm{rms}}/\overline{c}$ denotes the fluctuation Mach number and R_λ is a Reynolds number defined as $R_\lambda = u_{\mathrm{rms}}\lambda/\overline{v}$.

The numerical methodology to compute shock waves (see e.g. Hirsch 1990) has primarily been developed for steady aerodynamic flows, where the shock may be idealized as a discontinuity. Allowing physical viscosity to determine the shock-thickness in these flows would therefore be prohibitively expensive. Also, the Navier-Stokes equations themselves are generally considered invalid within shocks whose normal Mach number exceeds 2 (Sherman 1955). This has resulted in the popular use of "shock-capturing" schemes, in which numerical viscosity is used to smooth out the shock while ensuring that the jump conditions across the shock are satisfied. Equation 2 indicates that caution should be exercised when using shock-capturing schemes in turbulent flows. At low mean Mach numbers and turbulence Reynolds numbers, the shock thickness is seen to be comparable to the Kolmogorov scale. For example, if R_λ and M_t are 40 and 0.1 respectively, η/δ can be as low as 4, for a mean upstream Mach number of 1.5. Under these conditions, unless the local resolution is fine enough, a shock-capturing scheme would also dissipate the dynamically important scales of the turbulence, adversely influencing the computations.

Most schemes designed for steady aerodynamic flows are too dissipative for turbulence computations (see e.g. Hannappel et al 1995). Recent DNS (Lee et al 1994, Hannappel & Friedrich 1995, Mahesh et al 1997) have used the high-order, so-called essentially non-oscillatory (ENO) schemes (Harten & Osher 1987; Shu & Osher 1988, 1989) to treat the shock front. However, even ENO

schemes as high as sixth-order can be too dissipative for the turbulence (Lee et al 1997) if caution is not exercised. Current DNS of shock/turbulence interaction (Lee et al 1997, Mahesh et al 1997) restricted the shock-capturing algorithm to a small region around the shock wave (to capture the shock front distortion) and used local mesh refinement there to ensure that the shock-capturing did not significantly dissipate the turbulence. Figure 3 shows a result from Lee et al's (1997) computations.

2.5 *How High a* Re *Is High Enough?*

An acknowledged limitation of DNS is its restriction (by cost considerations) to low Reynolds number. This often leads to questions about the relevance of DNS to external aerodynamics. One hears astronomical estimates (based on $N \sim R_T^{9/4}$) for the computing time required should DNS be performed at real-life Reynolds numbers. There is the implicit assumption that for DNS to be useful at these high Reynolds numbers, they should be performed at similar Reynolds numbers. However, there are two questions that are not very often raised: "How high a Reynolds number is high enough?" and "What are the objectives of the computations?"

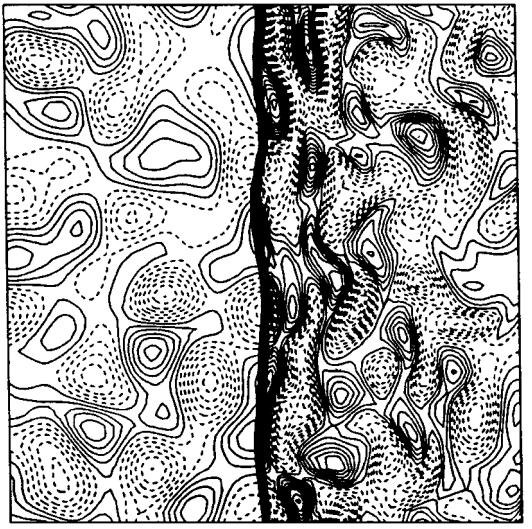

Figure 3 Contours of vorticity in the interaction of two-dimensional turbulence with a Mach-2 shock wave. The mean flow is from left to right. Solid and dashed lines correspond to positive and negative vorticity, respectively. The instantaneous shock front is illustrated by superposing contours of constant negative dilatation. Adapted from Lee et al (1997).

Consider the incompressible zero-pressure-gradient boundary layer. The Reynolds number dependence is commonly emphasized by noting that turbulence statistics, scaled in the conventional inner or outer variables, do not collapse at different Reynolds numbers. The mean velocity collapses well (see e.g. the review article by Fernholz & Finley 1996) for $R_\theta > 5000$, but collapse of the scaled turbulence stresses is unsatisfactory. Using arguments such as these to suggest that the flow is strongly Reynolds-number–dependent is perhaps misleading. The observed dependence on Reynolds number is a consequence of the scaling used; it does not imply that the essential physics has undergone significant change.

Compilation of data from a wide variety of experiments by Chapman (1979) shows a distinct separation between the energy-containing and dissipating scales, as proposed by Kolmogorov (1941). The small scales exhibit a universality (for energy) when scaled with Kolmogorov variables. The experimental data suggest that turbulent boundary layers scale in this manner at moderate Reynolds number. Fernholz & Finley (Figure 84, 1996) show that the streamwise spectrum of $\overline{u^2}$ at $y^+ = 200$ in a $R_\theta = 2470$ boundary layer exhibits a small subrange with $k^{-5/3}$ behavior. Also, when scaled with Kolmogorov variables, the spectrum collapses at the small scales with data obtained at Reynolds numbers greater by two orders of magnitude. Increasing the Reynolds number is seen merely to increase the extent of the $k^{-5/3}$ range. Note that $R_\theta = 2470$ is approximately a factor of two greater than Spalart's (1988) Reynolds number of 1410, a lot more comforting than the factors of 1000 that comparison to real-life Reynolds numbers would suggest is required.

The required separation between the energetic and dissipative scales is a matter of contention. Results from recent DNS (e.g. Kim et al 1987, Spalart 1988, Le & Moin 1994) suggest that accurate computation of the mean flow and second order statistics does not require significant scale separation. However, features that depend strongly on the smaller scales—such as intermittency or higher-order statistics—might require a wider separation for the results to hold at higher Reynolds number. As stated earlier, the purpose of the computations is an important question to raise. Our view of DNS is that of a research tool, and not a brute force solution to the Navier-Stokes equations for practical applications. The objective is not to reproduce real-life flows (say the flow over an airplane), but to perform controlled studies that allow better insight, scaling laws, and turbulence models to be developed.

The detailed Reynolds stress budgets from DNS provide valuable information on the relative magnitudes of the terms and their possible scaling. For example, the DNS of Kim et al (1987) in the plane channel, and the boundary layer of Spalart (1988) show that production balances dissipation near the wall, as

observed in experiments at significantly higher Reynolds numbers. The very low Reynolds number of the computation does not significantly influence this balance. Similarly the good correspondence of the structural features of the flow with high Reynolds number experiments, such as the near-wall streaks and the horseshoe vortices away from the wall, suggests that low Reynolds number computations might be adequate for the study of flow structures. If on the other hand one wanted to use DNS to rigorously verify local isotropy, as done experimentally by Saddoughi & Veeravalli (1994), there would be no choice but high Reynolds number computations. Similarly, free shear layers are known to possess critical Reynolds numbers at which their behavior undergoes significant change. Examples include the "mixing transition" in plane mixing layers at a vorticity thickness Reynolds number of about 5000. Such phenomena are clearly not amenable to Reynolds number scaling, and lower Reynolds number computations would be inadequate.

In summary, our response to the question "How high a *Re* is high enough?" would be "For what?" DNS need not obtain real-life Reynolds numbers to be useful in the study of real-life applications.

3. NOVEL NUMERICAL EXPERIMENTS

The term novel numerical experiments refers to computations in which the initial and/or boundary conditions are nonphysical in the sense that they are not readily attainable in laboratory experiments. The objective of these computations is to study in detail the influence of isolated physical parameters. Some examples of these numerical experiments follow.

3.1 *Forced Isotropic Turbulence*

Attempts by DNS to establish a subrange with $k^{-5/3}$ behavior in decaying isotropic turbulence have not been successful with as many as 128^3 points. Recall that the subrange separates the energy-containing and dissipating length scales. An interesting device has been used by computations seeking to establish a subrange—the largest resolved scales (typically the first two wavenumbers in the simulation) are externally forced. The proferred justification for such large-scale forcing is that if the range of scales being resolved is large enough, the details of the small scales should not depend upon the details of the forcing. Details of the forcing may vary (Eswaran & Pope 1988), but the underlying concept is the same: the forcing mimics the energy transfer to the inertial subrange from the larger energy-containing scales, that is, the large scales are modeled while the small scales are resolved (note the contrast to large eddy simulation). Spectra from forced computations display a noticeable subrange

with $k^{-5/3}$ behavior. Because the entire range of scales is not being resolved, higher Reynolds numbers are attained: Current 512^3 computations have a R_λ of nearly 200. An additional consequence of steady forcing is that the turbulence becomes statistically steady instead of decaying with time.

Forced computations have provided interesting insight into the physics of the small scales. A simple phenomenological picture of the regions of high vorticity and dissipation has emerged. Instantaneous fields from DNS (Siggia 1981; Kerr 1985; She et al 90; Vincent & Meneguzzi 1991, 1994; Ruetsch & Maxey 1991; Jiménez et al 1993) show that the regions of intense vorticity are essentially vortex tubes, as suggested by Kuo & Corrsin (1971). The radii and lengths of these vortex tubes scale with the Kolmogorov and integral length scales respectively, while their circulation appears to vary as $R_\lambda{}^{1/2}$. These vortex tubes have been shown to be a natural product of the turbulence evolution, and not a consequence of the forcing. They were found absent by She et al (1990) in a random Gaussian field with the same energy spectrum as a turbulent field. Despite their intense vorticity, the volume fraction occupied by the vortex tubes is small. As a result—and this is reminiscent of shocklets in compressible homogeneous turbulence (Section 5)—they do not contribute significantly to the overall dissipation. In an interesting demonstration of the relative insignificance of the vortex tubes to the overall kinetic energy evolution, Jiménez et al (1993) artificially removed the vortex tubes from their solution (R_λ was 96), switched off the large-scale forcing, and then compared the subsequent evolution of the flow to that in a computation where the tubes were retained. The decay rate of kinetic energy was seen to be identical in both computations.

Three-dimensional visualization of the vorticity and strain rate fields (R_λ was 83) was used by Kerr (1985) to suggest strong alignment between the vorticity and strain fields in the regions of intense vorticity. Probability distribution functions (PDFs) of the alignment between the vorticity vector and the eigenvectors of the strain rate tensor (Ashurst et al 1987) showed a strong tendency for the vorticity to align with the eigenvector corresponding to the intermediate eigenvalue. The largest compressive and extensional strains were seen to be perpendicular to the axis of the tubes, while a weak stretching was noted along the axis. A quantitative characterization of the tubes was provided by Ashurst et al (1987), who showed that the ratio of eigenvalues in the regions of intense dissipation was 1:3:-4, or one compressive and two extensional strains.

The physical picture that emerges from flow visualization and the PDFs is one of essentially two-dimensional vortices that are axially stretched. An interesting demonstration of this notion is provided by PDFs of the alignment

of the pressure gradient with strain-rate eigenvectors (Jiménez 1991). Conservation of angular momentum (Ashurst et al 1987) provides an explanation for the the tendency of the tubes to form when strain rate and vorticity are coupled. Modeling the vortex tubes as stretched vortices (Ashurst et al 1987, Jiménez 1991) also explains the observed ratio of eigenvalues.

Recent 512^3 computations at a R_λ of about 200 (Chen et al 1993, Wang et al 1996) have examined the hypotheses underlying the classical Kolmogorov-Obukhov (1962) theory of the inertial range. The theory, termed the refined similarity hypothesis (RSH), makes two assumptions: The velocity difference Δu_r over a distance r in the inertial range scales as $(r\epsilon_r)^{1/3}$, and the PDF of ϵ_r is log-normal (ϵ_r denotes the locally averaged dissipation). Some support for both hypotheses is provided by the computations.

The nonlinear terms in the Navier-Stokes equations transfer energy between different length scales. Details of the spectral transfer have been explored by DNS of forced turbulence (Domaradzki & Rogallo 1990, Yeung & Brasseur 1991, Ohkitani & Kida 1992, Zhou 1993). Of particular interest has been evaluating whether the transfer to a scale k is local (from scales of similar magnitude) or nonlocal (from scales of disparate magnitude). While experiments can measure the total energy transfer to a scale from other scales in the flow, details such as the exchange between prescribed scales are hard to measure. Such interactions can be computed by DNS, albeit at low Reynolds numbers. Individual triadic interactions (interaction between three Fourier modes) were examined by some of these studies. These can be misleading, however, since turbulent eddies are not simple Fourier modes. Analysis of the energy cascade requires summing the various triad interactions, and owing to the large cancellation among individual triads, the conclusions drawn depend strongly on which triads are summed. The Kolmogorov (1941) notion of local energy cascade in the inertial range is not supported (Yeung & Brasseur 1991) when individual triads are examined, but it is supported when contributions from all triads at a given scale disparity are summed (Zhou 1993).

A novel use of forced isotropic turbulence has been the study of fundamental issues pertaining to combustion. Flamelets (thin reacting regions) in premixed turbulent combustion were modeled by Girimaji & Pope (1992) as passive propagating surfaces, and their distortion by the turbulence examined. Such studies have allowed statistics of quantities such as the strain rate experienced by the flamelets and the evolution of their curvature to be obtained. Along similar lines, forced turbulence has allowed a detailed study of the turbulent distortion of material elements (Yeung et al 1990) and passive scalar mixing—recent studies include Pumir (1994), Jaberi et al (1996), Overholt & Pope (1996), and Juneja et al (1996).

3.2 *The Minimal Channel*

Insight into the dynamics of the near-wall region was provided by computations of the "minimal channel" by Jiménez & Moin (1991). This study demonstrated that the lower order statistics in the near-wall region ($y^+ < 40$) of channel flow could be reproduced by the dynamics of a model that was far simpler than the entire turbulent channel.

This simplified model was termed the minimal channel, and was obtained as follows. Channel-calculations were performed on domains significantly smaller than that of the entire turbulent channel. Statistics of the mean velocity, and turbulence intensity were then compared to those from the entire channel. Good agreement in the near-wall region ($y^+ < 40$) was observed for domain sizes greater than 100 wall units in the spanwise direction, and 250–350 wall units in the streamwise direction. Smaller domains were found unable to sustain the turbulence. The smallest domain that sustained the turbulence was termed the minimal channel.

The minimal channel represents a single unit of near-wall turbulence. It allows isolation of key structures and study of their dynamics. The good agreement of near-wall statistics despite significant disagreement in the outer region is an interesting demonstration of the weak statistical and dynamical dependence of the two regions. Another interesting observation is a very long ($Ut/h \approx 100$ where $U = 3Q/4h$, and h and Q denote the half-channel height and volume flux, respectively) cycle of intermittency, during which the turbulence intensities vary strongly. This regenerating cycle was proposed by Jiménez & Moin as the basis for sustenance of turbulence in the channel. Motivated by the flow structures in the minimal channel, Jiménez & Moin proposed a simple conceptual model for the dynamics of near-wall turbulence. Subsequent studies (e.g. Choi et al 1992, Carlson & Lumley 1996) have used the minimal channel to explore issues related to numerics and control, in a cost-effective manner.

3.3 *Shear-Free Boundary Layers*

A shear-free boundary layer is the boundary layer over a wall that is at rest relative to the free-stream. The turbulence in this boundary layer therefore evolves in the absence of mean shear. A solid wall influences the turbulence in its vicinity through two important mechanisms: mean shear, and zero penetration. The motivation behind studying shear-free boundary layers is to understand the influence of the zero penetration condition on the turbulence.

Shear-free boundary layers have been studied experimentally by Uzkan & Reynolds (1967) and Thomas & Hancock (1977), while Hunt & Graham (1978) have used linear analysis to theoretically predict their behavior. DNS of this flow was recently performed by Perot & Moin (1995a), who performed a further dissection of the influence of the wall. Three different wall boundary conditions were studied: a perfectly permeable wall (zero tangential velocity, periodic

normal velocity), an idealized free surface (zero normal velocity, zero normal gradients of tangential velocity), and a solid wall (no slip). The perfectly permeable wall and the idealized free surface allowed the effects of viscosity and kinematic wall blocking to be studied separately.

A noteworthy result of Perot & Moin's computations was insight into the influence of kinematic wall blocking. Prior to this study, the popular notion was that an impermeable wall would damp the wall-normal fluctuations to zero, thereby transferring energy to the tangential velocity components. The physical picture associated with this transfer was "splatting," where a blob of fluid in the free stream is squashed by the wall, and transfers energy from the normal to the tangential components. From the standpoint of the Reynolds averaged equations, splatting was associated with the near-wall reversal in the sign of the pressure-strain correlation in the equation for $\overline{v^2}$ (the wall-normal component of the Reynolds stress).

However, Perot & Moin found that the pressure-strain correlation was negligible in their Reynolds stress budgets of the idealized free surface. They suggested a phenomenological explanation based on visualization of the instantaneous flow field—"anti-splats," defined as fluid ejected away from the wall, thereby transferring energy from the horizontal to the vertical components of velocity. The pressure-strain correlation was postulated to be a result of the balance between splats and anti-splats, a balance that they showed *is governed by viscosity*. These phenomenological arguments were shown to hold in the vicinity of solid walls, and then used to develop a model for the slow pressure-strain correlation tensor (Perot & Moin 1995b). Flow visualization also inspired a new decomposition of inhomogeneous turbulence, which led to a model for the dissipation-rate anisotropy.

These computations are good examples of how numerical experiments can yield physical insight, which is then used to develop better turbulence models.

3.4 *The Interaction of Turbulence with Shock Waves*

The interaction of shock waves with supersonic turbulent boundary layers has proven difficult for turbulence models to predict. The experimental data show that the boundary layer may separate, that the turbulence levels amplify considerably, and that high levels of wall-pressure fluctuations exist in the vicinity of the shock. Shock wave/boundary layer interaction is influenced by the simultaneous presence of factors such as mean shear, bulk compression from the shock wave, inhomogeneous effects caused by the wall, mean streamline curvature, and unsteady effects caused by separation. Recent DNS has examined idealized problems that have allowed some of these effects to be studied in isolation. In particular, the influence of mean shear, upstream acoustic waves, and upstream entropy fluctuations (isobaric fluctuations in temperature and density) have been examined.

In order to study the influence of mean shear, Mahesh et al (1996) computed an idealized turbulent shear flow interacting with a Mach 1.2 normal shock. The mean velocity gradient and Mach number upstream of the shock wave were uniformly transverse to the shock front. This uniform mean Mach number allowed easier parameterization of the problem, while ensuring that the mean flow on both sides of the shock would essentially be in the x–direction. This idealized problem shows that while normal shocks amplify the kinetic energy of the turbulence, they suppress the Reynolds shear stress $\overline{uv}$. This effect is corroborated by linear analysis, which shows that vortex lines behind the shock wave would be closer to the vertical since the shock preferentially amplifies the transverse vorticity components. This would tend to decrease the magnitude of shear stress, a behavior not predicted by current Reynolds stress models.

DNS by Hannappel & Friedrich (1995) of isotropic turbulence interacting with a Mach 2 normal shock shows that acoustic waves in the upstream turbulence can lead to a suppression of kinetic energy amplification across the shock. They used this observation to suggest upstream acoustic waves as a possible reason for experiments in wind-tunnels reporting lower levels of kinetic energy amplification as compared to shock-tube experiments. This suppressing influence of upstream acoustic waves is consistent with linear analysis (Mahesh et al 1995), which shows that it is restricted to moderate mean upstream Mach numbers ($1.25-1.8$).

Turbulent velocity fluctuations stir up mean gradients in temperature and density to produce temperature and density fluctuations. These fluctuations, termed entropy fluctuations (Kovasznay 1953), are known to dominate the thermodynamic field in supersonic boundary layers. Experimental data (Fernholz & Finley 1981) show that the intensity (e.g. $T_{\rm rms}/\overline{T}$) of temperature and density fluctuations in boundary layers is comparable to that of the velocity field. DNS by Mahesh et al (1997) of Mach 1.3 and Mach 1.8 shocks shows that these upstream entropy fluctuations can significantly influence the turbulence evolution across shocks. In particular, the correlation between the upstream velocity and entropy field is important. Experimental data show that the correlation coefficient between streamwise velocity and temperature fluctuations is nearly -1 in adiabatic boundary layers. Negative upstream correlation strongly enhances amplification of the turbulence across the shock. On the other hand, positive upstream correlation reduces the kinetic energy amplification. The relative roles of bulk compression and baroclinic vorticity generation explain this behavior.

3.5 *The Far-Field of Turbulent Wakes*

Moser et al (1997) have recently examined the self-similarity of plane wakes in the far-field. The equations governing the first order moments for plane wakes

are known to admit self-similar solutions in the small-deficit limit, which is attained at large distances downstream of the body. Experiments (Wygnanski et al 1986, Marasli et al 1992) have shown that, despite the self-similarity of the mean velocity profile, quantities in the far-field such as the spreading rate and the Reynolds stresses are significantly affected by such factors as the body used, and two-dimensional forcing. This apparent dependence of the wake's self-similarity on its initial state was the focus of Moser et al's study.

DNS of temporally evolving wakes was performed, with three different initial conditions. The Reynolds number based on the integrated mass-flux deficit ($-\int_{-\infty}^{\infty}(U - U_\infty)\ \mathrm{d}y$) was 2000. Approximately 25 million points ($600 \times 260 \times 160$) were used to discretize the flow. An unforced wake was first computed as a baseline for comparison. This computation was initialized by using two instantaneous realizations of a turbulent boundary layer at a momentum thickness Reynolds number of 670 (Spalart 1988). The two other computations were those of two-dimensionally forced wakes; the initial conditions were the same as the unforced case except the two-dimensional modes of u and v were amplified by 5 and 20 in the two cases.

The simulations revealed the same trend as the experiments; i.e. self-similar states that depended strongly upon the initial conditions were obtained (Figure 4). The mean velocities from the three cases collapsed with each other, and with experiment (Weygandt & Mehta 1993) when plotted in similarity variables. The conventional scaling of the Reynolds stresses (using the maximum magnitude of the velocity deficit) did not collapse the data from the different computations, however; the Reynolds stresses in the forced wakes were almost an order of magnitude higher. The spreading rate was also observed to be different between the forced and unforced wakes. Similarity analysis of the mean momentum and Reynolds stress equations guided by the DNS data suggested alternative scalings that involved the spreading rate of the wake, and significantly improved the collapse of data from the different computations.

These computations are an example of how the strict control on the initial and boundary conditions afforded by DNS can be used to examine the dependence of a turbulent flow on its history or initial conditions.

3.6 *Active Control of Turbulent Flows*

The availability of detailed flow fields, and accurate control over the boundary conditions makes DNS a useful testbed to explore control strategies. We present here some examples that illustrate the use of DNS to control simple wall-bounded flows. The practical infeasibility of these examples puts them in the category of numerical experiments. These are essentially "what if"

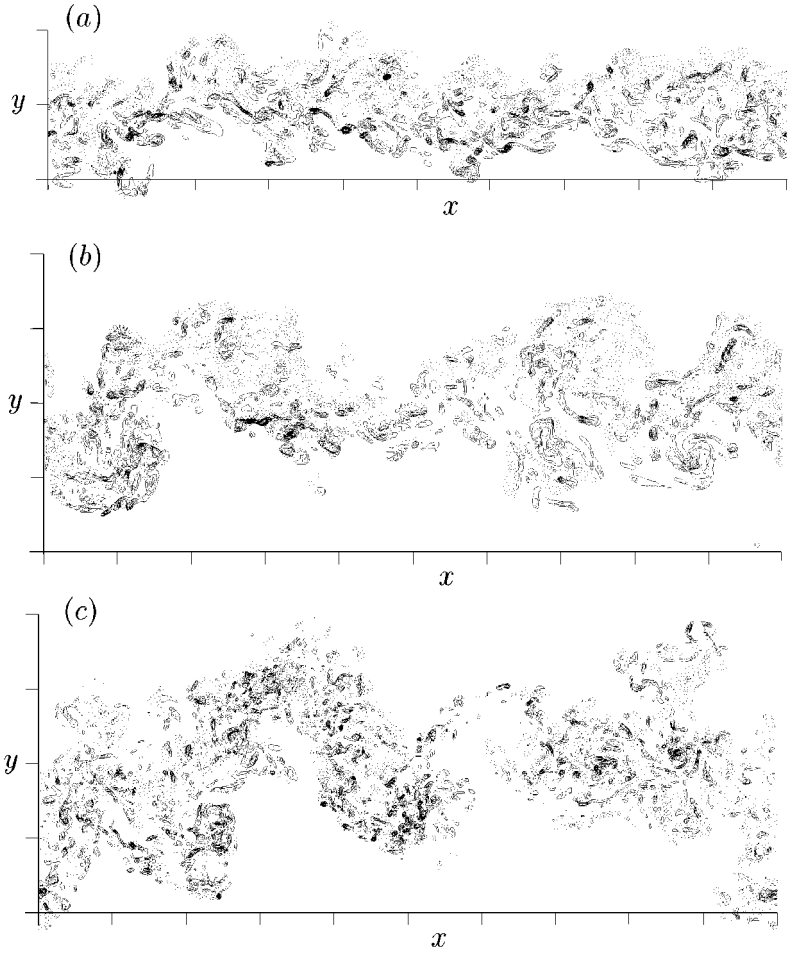

Figure 4 Contours of spanwise vorticity in an $x - y$ plane of a plane turbulent wake. The mean flow is from left to right. Solid and dashed lines correspond to positive and negative vorticity, respectively. (*a*) unforced wake; (*b*) and (*c*) wakes that are initially forced. Level of initial forcing is higher in (*c*) than in (*b*) . Adapted from Moser et al (1997).

experiments—the type that can be performed without concerns about hardware or implementation.

A study by Choi et al (1994) examined the efficacy of control applied at the wall in reducing friction drag in a turbulent channel. Their control strategy was motivated by past work that showed good correlation of near-wall streamwise vortices with Reynolds stress-producing events (Moin & Spalart 1987, Robinson 1991), and skin friction (Bernard et al 1993, Kravchenko et al

1993). The velocity at the wall was therefore controlled, with the objective of suppressing the sweep and ejection events associated with the streamwise vortices. It was shown that blowing and suction that was opposite in sign to the wall-normal velocity at $y^+ = 10$, i.e. $v_{\text{wall}}(x, z) = -v(x, y^+ = 10, z)$, reduced the drag by about 25%. The primary effect of the control was the lifting of high shear regions associated with sweeps, away from the wall. Of course, sensing the instantaneous velocity at $y^+ = 10$ and then applying control is not practical. What this study does demonstrate, however, is the feasibility of obtaining significant drag reduction in a fully-developed turbulent flow by controlling its relevant coherent structures.

Other control strategies based on manipulation of coherent structures have been explored by Carlson & Lumley (1996) and Jung et al (1992). Carlson & Lumley performed DNS in the minimal channel to evaluate the control, which was performed by a Gaussian-shaped actuator ($u = w = 0$, $v = \partial h/\partial t$, where h denotes the height of the actuator above the wall), at the wall. The location of the actuator with respect to the near-wall streaks (Kline et al 1967) was shown to influence the drag. Actuating the flow below low-speed streaks was observed to increase the drag, while actuation below high-speed streaks was seen to decrease it.

The possible use of new concepts, such as neural networks and control theory, to control turbulent flows is currently being explored. When Choi et al (1994) applied both sensing and control at the wall, the results were disappointing; the drag reduction dropped to 6%—about that obtained from passive control devices such as riblets. Control using wall-actuation alone requires some knowledge of how the wall-actuation influences the wall shear stress. A novel approach was developed by Lee et al (1997) who used DNS to train a neural network to approximate this influence and then provided the optimal wall-actuations that would minimize the drag. About 20 % reduction in drag was reported.

DNS is currently being used to explore an alternative strategy for control—the optimal control theory (Abergel & Temam 1990), which combines the tools of control theory with the Navier-Stokes equations. Conceptually, optimal control minimizes a cost functional which represents a combination of the quantity being controlled and the cost of control. Details of this procedure are outlined by Moin & Bewley (1995). Optimal control has the very attractive feature of rigor. Recent DNS has been quite useful in implementing and evaluating optimal control theory for wall-bounded flows. Computations by Moin & Bewley (1995) using optimal control and blowing and suction at the wall yielded 57% drag reduction in the turbulent channel at $Re_\tau = 100$ (the flow was relaminarized), significantly higher than that obtained from the ad hoc procedures described above. In the future, DNS is expected to play a central role in simplifying optimal control to where it can be implemented in practice.

4. SYNERGY WITH EXPERIMENTS

In this section we provide some examples of synergy between computation and experiment wherein they complement each other's strengths.

4.1 *Evaluation of Hot-Wire Response in Boundary Layers*

Moin & Spalart (1987) used DNS data from a turbulent boundary layer to estimate the accuracy of cross-wire probes and to quantify the magnitudes of the different sources of error. A model of a cross-wire to measure u and v, that is, with the wires in the x–y plane (plane of streamwise and wall-normal directions) was considered. The influence of the following assumptions (see Perry 1982) on the error was assessed: $u > 0$, negligible spanwise velocity, and linearized calibration based on assuming $v \ll u$. The influence of axial wire-cooling, the angle between the wires (120° as compared to 90°), flying the probe, and separation between the wires were also quantified. The results showed that neglecting the spanwise component of velocity was the most significant source of error. Increasing the wire angle to 120° reduced the error in all measured components by 25% to 50%. Flying the probe was also found to significantly reduce the error; the error was found to be less than 2% for a probe translating upstream at half the free-stream velocity.

A subsequent study by Suzuki & Kasagi (1992) used data from DNS of a turbulent channel (Kuroda 1990) to quantify the errors in near-wall hot-wire measurements. The influence of sensor length, sensor spacing, and neglect of the spanwise velocity component on the measurement accuracy were assessed, and a correction method involving two-point correlations of the velocity fluctuations was prescribed. DNS data from the turbulent channel (Hirschbirg 1992) was recently used by Pompeo & Thomann (1993), to explain why their four-wire probe yielded values for $\overline{vw}$ that were about 50% that of $\overline{uv}$, as opposed to being zero in a two-dimensional boundary layer. They then used a model of their probe to "make measurements" from DNS data. The computational study suggested that large instantaneous spanwise velocity gradients were likely responsible for the error in their measurements.

4.2 *Measurement of Vorticity*

DNS data has recently been used to provide probe design criteria and validate experimental measurements of vorticity in turbulent flows. Consider vorticity measurements made using thermal anemometry. Velocity data from a multi-sensor array of hot wires is differenced to obtain the velocity gradients, and thereby the vorticity. The length of the hot wires (denoted by L) and their separation distance (denoted by S) significantly influences the accuracy of the measurements. Analytical bounds on L and S were provided by Wyngaard (1969), who considered the response of a Kovasznay-type probe and a parallel

sensor probe (see the Annual Review article by Wallace and Foss 1995) to isotropic turbulence. Recently, Antonia et al (1993) used DNS data from the turbulent channel flow (Kim et al 1987) to evaluate both Wyngaard's analysis, as well as their experimental measurements. Values of $\partial u/\partial y$ from the experiments and computation were compared as a function of probe separation ($\Delta y = S$). Noticeable error was observed at very small and large separations. The error at large separations is of course anticipated since the approximation $\partial u/\partial y \approx \Delta u/\Delta y$, is only first order accurate in Δy. The error at small separations is a result of noise and calibration errors (Wallace & Foss 1995). Based on Antonia et al's comparison with DNS data, Wallace & Foss recommend an optimal separation distance of 2 to 4 times the Kolmogorov lengthscale.

Other experimental work has used data from DNS of the turbulent boundary layer (Spalart 1988), and the incompressible plane mixing layer (Rogers & Moser 1994) for validation of vorticity measurements in a similar manner (Figures 13 and 14 in Wallace & Foss 1995).

4.3 *The Backward Facing Step*

Le & Moin (1994) computed the turbulent flow over a backward facing step. When initiated, the objective of these computations was to generate a reliable database for a complex flow involving separation and reattachment. The initial computations had a Reynolds number (based on free-stream velocity and step height) of 5000, and expansion ratios ranging from 1.33 to 2. These computations exhibited mean velocity profiles that fell well below the log-law at distances as large as 19 step-heights downstream of the step. This result contradicted previous experimental studies (Westphal et al 1984, Kim et al 1978, Adams et al 1984) who reported recovery of the log-law as early as six step-heights downstream of the step (just downstream of reattachment). Two possible reasons for the discrepancy were conjectured. Lower Reynolds number in the computations was suggested, as usual, as one possible reason. The second conjecture was that the friction velocity in the experiments was incorrect because it was deduced from the Clauser chart, which implicitly assumes that the log-law holds.

Jovic & Driver (1994) tested these hypotheses. They performed experiments at the same Reynolds number and expansion ratio as the computations. Besides low Reynolds number, an added feature of the Jovic & Driver experiments was that the Clauser chart was not used. Instead, C_f was directly measured by a laser interferometer and used to obtain u_τ. These experiments confirmed that the computations were correct, that is, the mean velocity profiles did indeed fall below the log-law in the recovery region. The good agreement with the Jovic & Driver experiments established confidence in the computations while underscoring the impropriety of using the Clauser chart in regions of adverse pressure gradients.

4.4 *Near-Wall Measurements*

Kim et al (1987) performed DNS of the turbulent channel flow ($Re_c = 3300$). About four million grid points were used to resolve the flow. Extensive comparison of the results to experimental data was performed. In general, good agreement was found, but an important discrepancy was observed. Large differences in the turbulent intensity (rms velocity fluctuations normalized by local mean velocity) were observed in the near-wall region ($y^+ < 10$). The computed values of $u_{\rm rms}/U$ and $w_{\rm rms}/U$ approached 0.36 and 0.2 respectively at the wall, whereas the experimental values (Kreplin & Eckelmann 1979) were about 30 to 50 percent lower. Note that $\frac{\partial u}{\partial y}|_{\rm rms}/\frac{{\rm d}U}{{\rm d}y} \approx u_{\rm rms}/U$, and $\frac{\partial w}{\partial y}|_{\rm rms}/\frac{{\rm d}U}{{\rm d}y} \approx w_{\rm rms}/U$ at the wall.

Two experimental studies (Alfredsson et al 1988, Naqwi & Reynolds 1987) subsequently reexamined the near wall measurements of $\partial u/\partial y$ and $\partial w/\partial y$ in the channel, and found values very close to those obtained in the computations. Alfredsson et al (1988) obtained a value of 0.4 for $\frac{\partial u}{\partial y}|_{\rm rms}/\frac{{\rm d}U}{{\rm d}y}$ at the wall and estimated that $\frac{\partial w}{\partial y}|_{\rm rms}/\frac{{\rm d}U}{{\rm d}y}$ in their experiments was about 0.2. Their experiments showed that heat transfer to the fluid via the probe substrate caused significant differences between the static and dynamic responses of the probes when air or oil was used as the working fluid. They attributed the lower values in the previous experiments to the resulting error. Instead of using hot-film probes, Naqwi & Reynolds (1987) developed a laser wall-fringe-fan device. They obtained a value of 0.38 $\frac{{\rm d}U}{{\rm d}y}$ for $\frac{\partial u}{\partial y}|_{\rm rms}$ at the wall. Although unable to measure $\frac{\partial w}{\partial y}|_{\rm rms}$ sufficiently close to the wall, they reported that it was greater than or equal to 0.13 $\frac{{\rm d}U}{{\rm d}y}$ at the wall, in agreement with the computations.

In this example, the computations were used to critically examine experimental data, which then resulted in improved measurements. Since then, further validation of the DNS data has been provided by the experiments of Nishino & Kasagi (1989) using a three-dimensional particle tracking velocimeter, Niederschulte et al (1990) using LDV, and Durst et al (1995) using LDA. Existing DNS data for the turbulent channel is now considered reliable enough to be used as a benchmark by experimental diagnostic techniques (e.g. Durst et al 1996).

Near-wall values of the kurtosis of the wall-normal velocity have received recent attention. Computational values for the kurtosis [$\approx$22 in Kim et al's (1987) plane channel DNS and 19 in Eggels et al's (1994) DNS of pipe flow] are significantly higher than the values from experiments ($\approx$3 e.g. Durst et al 1995). A combined computational and experimental study by Xu et al (1996) examined this difference. Factors such as inadequate time resolution, implicit filtering during data collection and insufficient statistical accuracy were noted to make reliable near-wall measurements of kurtosis difficult. However, indirect

evidence for the accuracy of the computational values was offered. Data from DNS of the turbulent channel was first used to determine the signature of events that contributed to the high kurtosis. It was determined that events with large values of $|v'/v_{\text{rms}}|$ only occurred in the near-wall region ($y^+ < 10$). Pipe flow experiments with accurate near-wall measurements were then performed and the data examined for events with a signature similar to the computations. The experimental data were found to be consistent with the DNS, suggesting that the high near-wall values of the kurtosis were physical in origin.

5. TURBULENCE MODELING

Some of the most important contributions of DNS have been in phenomenological modeling for engineering applications. The Reynolds stress equations, which form the basis for closure of the Reynolds averaged mean flow equations, contain several terms that must be modeled but are difficult to measure experimentally. For example, the pressure-strain correlation tensor, which is of comparable magnitude to the production terms, has not been amenable to measurement. Similarly, measurements of the dissipation typically require the assumption of isotropy. This is not so in DNS: All the terms in the Reynolds stress equations can be directly computed (Figure 5).

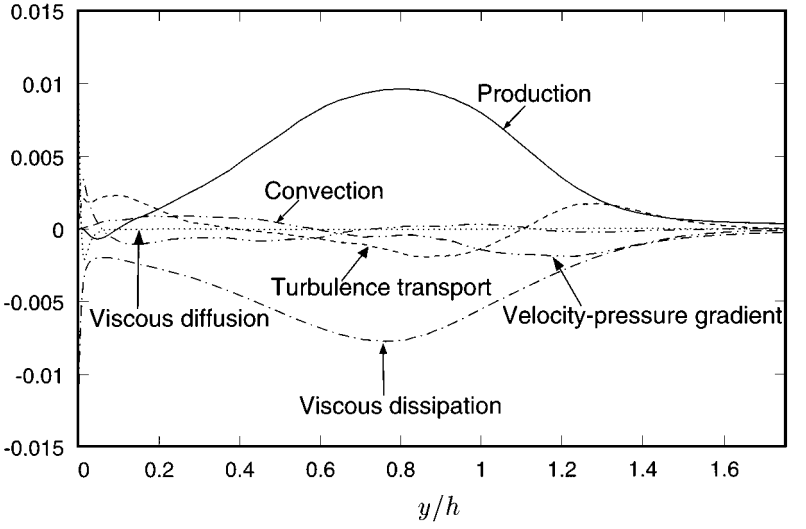

Figure 5 The budget of turbulent kinetic energy as a function of wall-normal distance in the turbulent flow over a backstep. All quantities are normalized by U_0^2/h, where U_0 is the freestream velocity and h is the step height. Adapted from Le & Moin (1994).

Historically, Rogallo's (1981) DNS of homogeneous turbulence was the first to provide complete Reynolds stress budgets for a turbulent flow. He used the data to evaluate models for the pressure-strain correlation and dissipation. Since then, DNS data for homogeneous shear flow (Rogers et al 1986) and axisymmetrically strained flow (Lee & Reynolds 1985) have been widely used to test models (Hunt 1988, Speziale 1994, Shih 1996). DNS data from wall-bounded flows have been very useful in providing the near-wall behavior of the terms in the budget. In fact, the first computed budgets in the plane channel (Mansour et al 1988) revealed significant near-wall error in the kinetic energy budgets derived from Laufer's (1955) classical pipe flow experiments (Figure 5.5 in Townsend 1976).

In the absence of DNS data, the testing of models is somewhat indirect. For example, a proposed model for the pressure-strain correlation would be combined with existing models for the other terms, and then results for quantities such as the pressure coefficient, C_p, or the skin-friction coefficient, C_f, would be compared to experiment. DNS allows more direct testing of models: A model for the pressure-strain correlation can be evaluated by direct comparison to DNS values of the pressure-strain correlation. Suggestions such as Durbin's (1991) proposal that $\overline{v^2}$, and not the turbulent kinetic energy k, provides the relevant velocity scale for the eddy-viscosity in wall-bounded flows (i.e., $\nu_t = C_\mu \overline{v^2} T$ where T is a turbulence time scale) can be directly tested (see e.g. Rodi & Mansour 1993) by computing C_μ and examining its spatial constancy.

If a model is found to perform unsatisfactorily (or satisfactorily for that matter), answers to the query "why ?" may be sought. A study by Bradshaw et al (1987) provides a good example. This study examined a central assumption made by models for the rapid pressure-strain correlation. The so-called rapid pressure in incompressible flows is given by the relation,

$$p_{\text{rapid}} = -\frac{1}{4\pi} \int_V 2 \frac{\partial U_i}{\partial x_j} \frac{\partial u'_j}{\partial x_i} \, G \, dV, \tag{3}$$

where G denotes the Green's function of the Laplacian. The rapid pressure therefore depends on the *volume integral* of the mean velocity gradient weighted by the fluctuating gradients. However, in deriving models for the pressure-strain correlation, it is often assumed that p_{rapid} only depends upon the *local* mean velocity gradient; i.e. the mean velocity gradient is taken out of the integral in Equation 3. The appropriateness of this assumption was tested by Bradshaw et al (1987) in the turbulent channel. The pressure-strain correlation computed using the pressure obtained from the local approximation was compared to its exact value. The local approximation was seen to perform well outside of the viscous sublayer. The correlation of the rapid pressure with its Laplacian was then examined and found to be high, suggesting a possible explanation for this

success. The inadequacy of the approximation in the sublayer was explained by noting that the mean velocity in that region varied over a distance comparable to the correlation length of the fluctuating gradient.

The availability of DNS data has resulted in novel approaches to model evaluation. Parneix et al (1996) used an a priori test to evaluate a second moment closure model applied to the flow over a backstep. The various equations in the model were individually tested by solving the model equations for one variable, while fixing the other variables to their DNS values. Such evaluation for the backstep showed that contrary to popular belief the much-maligned ϵ equation performed remarkably well; the model equation for $\overline{uv}$ was the weak link.

Similarly, DNS allows testing of the concepts behind a model. Compressible turbulence provides a good example. The growth rate of compressible mixing layers has been shown by experiments (e.g. Brown & Roshko 1974) to be lower than that of their incompressible counterparts. Motivated by computations of two-dimensional forced mixing layers, which showed the formation of shock waves between the Kelvin-Helmholtz rollers, Zeman (1990) proposed a phenomenological model for this trend. He contended that at high speeds "shocklets" form in mixing layers; the large gradients in these shock waves lead to increased dissipation of the turbulence (manifested by the dilatation dissipation), and hence lower growth rate of the mixing layer. Zeman's model showed good agreement with experimental data for the growth rate. DNS of homogeneous compressible shear flow (Blaisdell et al 1993, Sarkar et al 1991) showed a similar suppression of turbulence growth rate with increased compressibility. The DNS database was therefore used by Blaisdell & Zeman (1992) to test the dynamical significance of shocklets. Instantaneous snapshots and time evolution of the dilatation dissipation showed that shocklets occurred too infrequently to make a significant contribution to the dilatation dissipation. Most of the dilatation dissipation arose from large scale acoustic waves; that is, while Zeman's model predictions were correct the background phenomenology was not.

The early DNS were of simple flows, which turbulence models had already been calibrated for and could predict successfully. As a result, their impact was not very pronounced. Currently, however, flows that models are experiencing difficulty with are being computed. Turbulence under mean rotation is a good example. A large amount of experimental and theoretical attention has been devoted to the subject because of applications such as turbomachinery, geophysical flows, and internal combustion engines. In practical flows, rotation is complicated by the presence of factors such as body forces other than the Coriolis force, mean gradients, and wall effects. DNS has been used to study homogeneous rotating turbulence, and in the process isolate the influence

of rotation. The subject is fairly rich—recent publications by Bartello et al (1994) and Cambon et al (1997) review earlier work. The focus of most studies has been to determine the conditions under which mean rotation produces anisotropy in initially isotropic turbulence. The DNS results have been used to parameterize this influence in turbulence models, which have then been applied to complex flows involving strong rotation.

Other computed flows where models experience difficulty include the three-dimensional turbulent boundary layer (Moin et al 1990), separated flows such as the flow over a backstep (Le & Moin 1994), and pressure-gradient–driven separation on a flat plate (Na & Moin 1996). Compressible turbulent channel flow (Coleman et al 1995) and shock/turbulence interaction (Lee et al 1993, 1994; Mahesh et al 1997) are additional examples.

6. BOUNDARY LAYER STRUCTURE

Perhaps the most tangible contribution of DNS to our understanding of turbulent boundary layers has been in providing a more realistic view of its structure. Early simulations of wall-bounded flows were performed at a time (early 1980s) when interest in coherent structures was at its peak among the research community. Most of what was known about boundary layer structure then (e.g. see the review by Cantwell 1981) was deduced from experiments, with much extrapolation from incomplete data. The early large eddy simulation (LES) (Moin & Kim 1982; Kim 1983, 1985) first reproduced classical experimental results such as the pulsed hydrogen bubble experiments of Kline et al (1967) and the VITA technique of Blackwelder & Kaplan (1976). Access to velocity, pressure, and vorticity fields in three-dimensional space and time allowed DNS to fill in the gaps in the popular notions of boundary layer structure. In retrospect, this use of DNS represented a major change in the accepted role of computations in turbulence research. Instead of merely predicting experimentally measured statistical correlations, as was common in the engineering research community, computations were now being used to yield information impossible to obtain from experiments. The confidence in DNS data has progressed to the point where modern ideas on coherent structures such as the critical-point notions of Chong et al (1990) are routinely evaluated using DNS data (Cantwell et al 1997).

Some of the insights into boundary layer structure gained from DNS are summarized below (see also Moin & Spalart 1987, Robinson 1991). First consider the turbulence in the near-wall region. The velocity vectors in any vertical plane normal to the mean flow (y–z) direction show an abundance of quasi-streamwise vortices in the near-wall region. These vortices are associated with intense velocity fluctuations and large skin friction at the wall (Bernard et al

1993, Kravchenko et al 1993). They have also been shown to be responsible for turbulence generation. The so-called "bursting" event (Kline et al 1967) which was once considered a central feature in turbulence regeneration may not be as profound an occurrence as was once thought. DNS data suggests that the observed bursting event may simply be due to the passage of streamwise vortices past the measuring station (Kim & Moin 1986). The signature of a burst as reported in experiments by Kline et al (1967) was the lifting of dye from the near wall region, oscillation of its trace, and eventual breakdown. Probe measurements also showed that the bursts were associated with high Reynolds shear stress. Kim & Moin (1986) demonstrated that these events could be reproduced by the simple passage of a streamwise vortex over a region of dye concentration near the wall.

The then-prevalent notion of near-wall structure was that the wall layer was composed of alternating arrays of elongated counter-rotating streamwise vortices surrounding the wall-layer streaks. The DNS data showed that this was not true. Although the wall layer is composed of elongated regions of high-speed and low-speed streamwise velocity, the same is not true of streamwise vorticity. The streamwise extent of the vortices in the near-wall region is much shorter (400 wall units), and they are not necessarily in pairs. The large streamwise length of the streaks (as seen in contours of constant u') appears to be due to a sequence of vortices following each other, pumping high-speed fluid toward the wall and low-speed fluid away from the wall (Sendstad & Moin 1992). Plots of velocity vectors in planes perpendicular to the mean flow direction along a randomly chosen low speed streak in turbulent channel flow are shown in Figure 6. Note that the vortices seen near the streak have alternate signs, and that the distance between the vertical planes is slightly more than 350 wall units.

Consider the turbulence outside the near-wall region. Away from the wall, histograms of the inclination angle of the vorticity vector clearly indicate (Moin & Kim 1985) the predominance of vortical structures inclined at 45° to the wall, as hypothesized three decades earlier by Theodorssen (1955), and later substantiated in laboratory visualizations by Head & Bandyopadhay (1981). Two-point correlation functions with directions of probe separation along various inclination angles to the wall also provide strong statistical support for the dominance of hairpin-like structures inclined at 45° to the wall. Vortex lines drawn in instantaneous flow fields show hairpin-like structures; however, often the hairpins are not symmetric, having only one clearly identifiable leg.

The channel flow computations revealed that the hairpin vortices were often formed by the rollup of spanwise sheets of vorticity *away* from the wall. This observation resulted in the conjecture that hairpin vortices were simply a result of turbulent fluctuations perturbing the spanwise vorticity associated with the mean shear and the stretching of these fluctuations by the mean strain

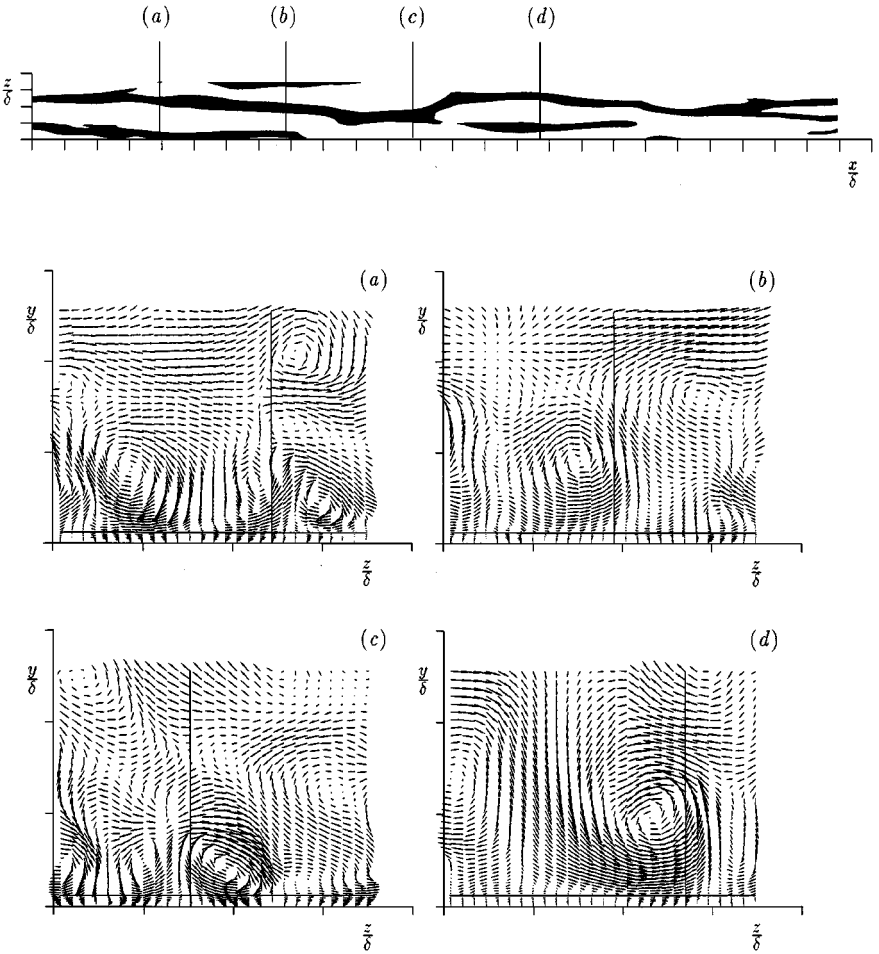

Figure 6 Velocity vectors in vertical planes along a randomly chosen low-speed streak at $y^+ = 5$. Figure displays regions where $u' < -u_\tau$ (top). Vertical lines show the location of the long low-speed streak in the topmost figure. Horizontal line is the plane of the streak ($y^+ = 5$). This illustrates that streaks are maintained by a system of staggered vortices. Tick marks are 0.25 units apart except on the horizontal axis of the figure where they are 0.5 units apart (*top*). From Sendstad & Moin (1992).

rate. That is to say, hairpin vortices were a consequence of mean shear, and inhomogeneous effects caused by the wall were not a necessary ingredient in their formation. The homogeneous shear simulations of Rogers & Moin (1987) proved this conjecture to be correct. The value of Sq^2/ϵ (S, q^2, and ϵ denote the mean velocity gradient, the trace of the Reynolds stress tensor, and the kinetic energy dissipation, respectively) in the homogeneous shear computation were matched to that in the log-region of the channel. Diagnostics similar to those used in the channel flow were then used to demonstrate the presence of hairpin vortices inclined at about 45 degrees to the mean flow direction. Inclined vortical structures in homogeneous shear flow were also observed by Kida & Tanaka (1994), who pointed out that the distance between them is determined by the length scale of the initial vorticity fluctuations. Also, a plausible mechanism for the generation and interaction of the vortical structures was proposed. The Reynolds stresses and the structure of turbulent shear flows depend on Sq^2/ϵ. Sq^2/ϵ in the near-wall region of channel flow is about 35, as compared to 7 in the log-region. Computations of homogeneous shear flow at high shear rates ($Sq^2/\epsilon \approx 34$) by Lee et al (1990) show the presence of streaks remarkably similar to those in the near wall region of the turbulent channel, suggesting that the presence of streaks may also be attributed solely to the mean shear.

DNS has also helped resurrect some early concepts that had not been properly evaluated because of insufficient data. A couple of examples are provided below. In the mid 1980s there were concerns about the objectivity of the various accounts of coherent structures based on flow visualizations and a lack of an apparent link between such observations and quantitative models of turbulence. Two decades earlier, Lumley (1967) had proposed an attractive definition of coherent structures as the eigenfunctions of the two-point velocity correlation tensor. Lumley's definition (formulated in terms of the proper orthogonal decomposition, or POD) expressed the turbulent velocity field as a superposition of these deterministic structures with random coefficients. Moin & Moser (1989) computed the complete (*four dimensional*) two-point correlation tensor in turbulent channel flow and extracted its eigenfunctions. The resulting dominant characteristic eddy was found to contribute as much as 76% of the total turbulent kinetic energy, and even more to turbulence production. The dominant characteristic eddy consisted of a pair of counter-rotating vortices inclined with respect to the wall.

One of the more common approaches to coherent structure analysis is the conditional averaging method. Conditional averages can be approximated using the two-point correlation tensor in conjunction with the mean square estimation technique. The governing equation for the joint probability density function for the velocity and deformation tensors contains conditional eddies, and therefore provides a linkage between turbulence modeling and organized structures.

Using DNS data of homogeneous shear flow, Adrian & Moin (1988) provided a detailed evaluation of the stochastic estimation technique for the detection of instantaneous turbulent structures. By combining this technique with probability density functions computed using the same database, they were able to identify the most frequently occurring structures and those that contribute most to turbulence production.

7. CONCLUDING REMARKS

The contributions of direct numerical simulations to turbulence research in the last decade have been impressive. The availability of raw DNS data has spawned a new trend in the field: It has brought together researchers from diverse disciplines and with diverse viewpoints (e.g. see Hunt 1988). Although generating data can be time-consuming, analyzing stored data requires only modest resources. New ideas and theories can therefore be readily tested.

The future of DNS in turbulence research appears bright. In our opinion, the greatest strength of DNS is the stringent control it allows over the flow being studied. Exploiting this strength and using it to examine idealized flows such as those discussed in Section 3 is how DNS is likely to be most useful. The fundamental areas of aeroacoustics, flow control, high-speed flows, and reacting flows will likely see significant progress in the next decade. Given the current trends in computer hardware, the Reynolds numbers in these computations will at best be modest. The increased computer power will likely be used to improve statistical samples, and to consider a wider range of other physical parameters.

The Reynolds numbers of the simpler turbulent flows are currently approaching those of the smaller-scale experiments. As an example, the classical experiments on decaying grid turbulence by Comte-Bellot & Corrsin (1971), were recently computed by AA Wray (unpublished information). The computations were performed on a parallel machine using a 512^3 grid. Excellent agreement with the experiment was obtained. A novelty of these computations was that the computed range of scales was actually greater than that measured experimentally. DNS of forced isotropic turbulence has been conducted on 512^3 grids by several workers (Jiménez et al 1993, Chen et al 1993, Wang et al 1996) interested in the behavior of the small scales. The Reynolds number in these computations actually exceeds that in most laboratory experiments.

As the flow geometries become more complex, the numerical methods used in DNS will have to evolve. The computational fluid dynamics community has much experience with complex geometries, and much can be learned about gridding techniques from them. However, the significantly higher numerical fidelity required by DNS must be kept in mind. The analysis and development of current numerical schemes is largely based on linear equations such as the

advection and diffusion equations. Nonlinear methods of analysis (e.g. Ghosal 1996) and development are likely to prove very productive. From the standpoint of computer hardware, parallel computing appears to be the enabling technology for the next generation of archivable simulations. A significant amount of the time taken by DNS is spent in computing statistics: As shown by Carati et al (1996), one of the effective uses of parallel machines is to simultaneously compute an ensemble of flows, thereby reducing the overall turnaround time.

ACKNOWLEDGMENTS

This article is dedicated to the memory of Dean R Chapman (1922–1995), whose inspirational leadership and vision led to the development of the computational turbulence research program at NASA Ames and Stanford. We are also grateful to the United States Air Force Office of Scientific Research, the Office of Naval Research, and NASA for their sustained support of the turbulence research program at Stanford. Reviewing a review can be arduous; we are thankful to Dr. Robert Rogallo and to Professors Bradshaw and Lele for reviewing a draft of ours.

Visit the *Annual Reviews home page* at http://www.AnnualReviews.org.

Literature Cited

Abergel F, Temam R. 1990. On some control problems in fluid mechanics. *Theor. Comput. Fluid Dyn.* 1:303–25

Adams EW, Johnston JP, Eaton JK. 1984. Experiments on the structure of turbulent reattaching flow. *Rep. MD-43*, Thermosci. Div., Dept. Mech. Eng., Stanford Univ., Calif.

Adrian RJ, Moin P. 1988. Stochastic estimation of organized turbulent structure: homogeneous shear flow *J. Fluid Mech.* 190:531–59

Akselvoll K, Moin P. 1996. Large-eddy simulation of turbulent confined coannular jets. *J. Fluid Mech.* 315:387–411

Alfredsson PH, Johansson AV, Haritonidis J, Eckelmann H. 1988. The fluctuating wall-shear stress and the velocity field in the viscous sublayer. *Phys. Fluids* 31:1026–33

Antonia RA, Zhu Y, Kim J. 1993. On the measurement of lateral velocity derivatives in turbulent flows. *Exp. Fluids* 15:65–69

Ashurst WT, Kerstein AR, Kerr RM, Gibson CH. 1987. Alignment of vorticity and scalar gradient with strain rate in simulated Navier-Stokes turbulence. *Phys. Fluids* 30:2343–53

Bartello P, Métais O, Lesieur M. 1994. Coherent structures in rotating three-dimensional turbulence. *J. Fluid Mech.* 273:1–29

Bernard PS, Thomas JM, Handler RA. 1993. Vortex dynamics in near-wall turbulence. In *Near-Wall Turbulent Flows*, ed. RMC So, CG Speziale, BE Launder, pp. 43–52. New York: Elsevier

Blaisdell GA, Mansour NN, Reynolds WC. 1993. Compressibility effects on the growth and structure of homogeneous turbulent shear flow *J. Fluid Mech.* 256:443–85

Blaisdell GA, Spyropoulos ET, Qin JH. 1996. The effect of the formulation of nonlinear terms on aliasing errors in spectral methods. *Appl. Num. Math.* 21:207–19

Blaisdell GA, Zeman O. 1992. Investigation of the dilatational dissipation in compressible homogeneous shear flow. *Proc. Cent. Turbul. Res., Summer Program, Stanford, 1992*, pp. 231–45. Stanford: CTR

Blackwelder RF, Kaplan RE. 1976. On the wall structure of the turbulent boundary layer. *J. Fluid Mech.* 76:89–112

Bradshaw P. 1994. Turbulence: the chief outstanding difficulty of our subject. *Exp. Fluids* 16:203–16

Bradshaw P, Mansour NN, Piomelli U. 1987. On local approximations of the pressure-strain term in turbulence models. *Proc. Cent. Tur-*

bul. Res., Summer Program, Stanford, 1987, pp. 159–64. Stanford: CTR
Brown G, Roshko A. 1974. On density effects and large structure in turbulent mixing layers. *J. Fluid Mech.* 64:775–816
Cambon C, Mansour NN, Godeferd FS. 1997. Energy transfer in rotating turbulence. *J. Fluid Mech.* 337:303–22
Cantwell BJ. 1981. Organized motion in turbulent flow. *Annu. Rev. Fluid Mech.* 13:457–515
Cantwell BJ, Chacin JM, Bradshaw P. 1997. On the dynamics of turbulent boundary layers. In *Self-Sustaining Mechanisms of Wall Turbulence*, ed. R Panton. Ashurst, UK: Comput. Mech. In press
Canuto C, Hussaini MY, Quarteroni A, Zang TA. 1988. *Spectral Methods in Fluid Dynamics.* Berlin: Springer
Carati D, Wray A, Cabot W. 1996. Ensemble averaged dynamic modeling. *Proc. Cent. Turbul. Res., Summer Program, Stanford, 1996*, pp. 237–48. Stanford: CTR
Carlson HA, Lumley JL. 1996. Active control in the turbulent wall layer of a minimal flow unit. *J. Fluid Mech.* 329:341–71
Chapman DR. 1979. Dryden Lecture: Computational aerodynamics development and outlook. *AIAA pap. 79–0129R*
Chen S, Doolen GD, Kraichnan RH, She Z-S. 1993. On statistical correlations between velocity increments and locally averaged dissipation in homogeneous turbulence. *Phys. Fluids A* 5:458–63
Choi H, Moin P, Kim J. 1992. Turbulent drag reduction: studies of feedback control and flow over riblets. *Rep. TF-55*, Thermosci. Div., Dept. Mech. Eng., Stanford Univ., Calif.
Choi H, Moin P. 1994. Effects of the computational time step on numerical solutions of turbulent flow *J. Comp. Phys.* 113:1–4
Choi H, Moin P, Kim J. 1994. Active turbulence control for drag reduction in wall-bounded flows. *J. Fluid Mech.* 262:75–110
Chong MS, Perry AE, Cantwell BJ. 1990. A general classification of three-dimensional flow fields. *Phys. Fluids A* 2:765–77
Coleman GN, Kim J, Moser RD. 1995. A numerical study of turbulent supersonic isothermal-wall channel flow. *J. Fluid Mech.* 305:159–83
Comte-Bellot G, Corrsin S. 1971. Simple Eulerian time correlation of full- and narrow-band velocity signals in grid-generated "isotropic" turbulence. *J. Fluid Mech.* 48:273–337
Corral R, Jiménez J. 1995. Fourier/Chebychev methods for the incompressible Navier-Stokes equations in infinite domains. *J. Comp. Phys.* 121:261–70
Domaradzki JA, Rogallo RS. 1990. Local energy transfer and nonlocal interactions in homogeneous isotropic turbulence. *Phys. Fluids A* 2:413–26
Durbin PA. 1991. Near-wall turbulent closure modeling without "damping functions." *Theor. Comput. Fluid Dyn.* 3:1–13
Durst F, Jovanović J, Sender J. 1995. LDA measurements in the near-wall region of a turbulent pipe flow. *J. Fluid Mech.* 295:305-35
Durst F, Kikura H, Lekakis I, Jovanovic J, Ye Q. 1996. Wall shear stress determination from near-wall mean velocity data from turbulent pipe and channel flows. *Exp. Fluids* 20:417–28
Eggels JGM, Unger F, Weiss MH, Westerweel J, Adrian RJ, et al. 1994. Fully developed turbulent pipe flow: a comparison between direct numerical simulation and experiment. *J. Fluid Mech.* 268:175–209
Erlebacher G, Hussaini MY, Kreiss HO, Sarkar S. 1990. The analysis and simulation of compressible turbulence. *Theor. Comput. Fluid Dyn.* 2:73–95
Eswaran V, Pope SB. 1988. An examination of forcing in direct numerical simulations of turbulence. *Comput. Fluids* 16:257–78
Feiereisen WJ, Reynolds WC, Ferziger JH. 1981. Numerical simulation of a compressible homogeneous turbulent shear flow. *Rep. TF-13*, Thermosci. Div., Dept. Mech. Eng., Stanford Univ., Calif.
Fernholz HH, Finley PJ. 1981. A further compilation of compressible boundary layer data with a survey of turbulence data. *AGARDograph 263*
Fernholz HH, Finley PJ. 1996. The incompressible zero-pressure gradient turbulent boundary layer: an assessment of the data. *Prog. Aerosp. Sci.* 32:245–311
Fox DG, Lilly DK. 1972. Numerical simulation of turbulent flows. *Rev. Geophys. Space. Phys.* 10:51–72
Ghosal S. 1996. An analysis of numerical errors in large-eddy simulations of turbulence. *J. Comp. Phys.* 125:187–206
Girimaji SS, Pope SB. 1992. Propagating surfaces in isotropic turbulence. *J. Fluid Mech.* 234:247–77
Hannappel R, Friedrich R. 1995. Direct numerical simulation of a Mach 2 shock interacting with isotropic turbulence. *Appl. Sci. Res.* 54:205–21
Hannappel R, Hauser T, Friedrich R. 1995. A comparison of ENO and TVD schemes for the computation of shock-turbulence interaction. *J. Comp. Phys.* 121:176–84
Harten A, Osher S. 1987. Uniformly high-order accurate nonoscillatory schemes, I. *SIAM J. Num. Anal.* 24:279–309
Head MR, Bandopadhyay P. 1981. New aspects of the boundary layer structure. *J. Fluid Mech.* 107:297–338

Hirsch C. 1990. *Numerical Computation of Internal and External Flows: Vol. 2*. West Sussex, UK: Wiley
Hirschberg S. 1992. *Direkte Simulation der turbulenten Taylor-Couette Strömung und der ebenen Kanalströmung*. Diss. Pap., ETH, Zürich, Nr. 9912
Hunt JCR. 1988. Studying turbulence using direct numerical simulation: 1987 Center for Turbulence Research NASA Ames/Stanford Summer Programme. *J. Fluid Mech.* 190:375–92
Hunt JCR, Graham JMR. 1978. Free-stream turbulence near plane boundaries. *J. Fluid Mech.* 84:209–35
Jaberi FA, Miller RS, Madnia CK, Givi P. 1996. Non-Gaussian scalar statistics in homogeneous turbulence. *J. Fluid Mech.* 313:241–82
Jiménez J. 1991. On small scale vortices in turbulent flows. *Phys. Fluids A* 4:652–54
Jiménez J, Moin P. 1991. The minimal flow unit in near-wall turbulence. *J. Fluid Mech.* 225:213–40
Jiménez J, Wray AA, Saffman PG, Rogallo RS. 1993. The structure of intense vorticity in isotropic turbulence. *J. Fluid Mech.* 255:65–90
Jovic S, Driver DM. 1994. Backward-facing step measurement at low Reynolds number, $Re_h = 5000$. *NASA TM 108807*
Juneja A, Pope SB. 1996. A DNS study of turbulent mixing of two passive scalars. *Phys. Fluids* 8:2161–84
Jung WJ, Mangiavacchi N, Akhavan R. 1992. Suppression of turbulence in wall-bounded flows by high-frequency spanwise oscillations. *Phys. Fluids A* 4:1605–7
Kasagi N, Tomita Y, Kuroda A. 1992. Direct numerical simulation of the passive scalar field in a turbulent channel flow. *ASME J. Heat Trans.* 14:598–606
Kerr RM. 1985. Higher-order derivative correlations and the alignment of small-scale structures in isotropic numerical turbulence. *J. Fluid Mech.* 153:31–58
Kida S, Tanaka M. 1994. Dynamics of vortical structures in a homogeneous shear flow. *J. Fluid Mech.* 274:43–68
Kim J, Kline SJ, Johnston JP. 1978. Investigation of separation and reattachment of a turbulent shear layer: flow over a backward-facing step. *Rep. MD-37*, Thermosci. Div., Dept. Mech. Eng., Stanford Univ., Calif.
Kim J. 1983. On the structure of wall-bounded turbulent flows. *Phys. Fluids* 26:2088–97
Kim J. 1985. Turbulent structures associated with the bursting event. *Phys. Fluids* 28:52–58
Kim J, Moin P. 1986. Flow structures responsible for the bursting process. *Bull. Am. Phys. Soc.* 31:1716 (Abstr.)
Kim J, Moin P, Moser RD. 1987. Turbulence statistics in fully-developed channel flow at low Reynolds number. *J. Fluid Mech.* 177:133–66
Kleiser L, Zang TA. 1991. Numerical simulation of transition in wall-bounded shear flows. *Annu. Rev. Fluid Mech.* 23:495–537
Kline SJ, Reynolds WC, Schraub FA, Rundstadler PW. 1967. The structure of the turbulent boundary layer. *J. Fluid Mech.* 30:741–73
Kovasznay LSG. 1953. Turbulence in supersonic flow. *J. Aero. Sci.* 20:657–82
Kravchenko AG, Choi H, Moin P. 1993. On the relation of near-wall streamwise vortices to wall skin friction in turbulent boundary layers. *Phys. Fluids A* 5:3307–9
Kravchenko AG, Moin P. 1997. On the effect of numerical errors in large eddy simulations of turbulent flows. *J. Comp. Phys.* 131:310–22
Kreplin H, Eckelmann H. 1979. Behavior of the three fluctuating velocity components in the wall region of a turbulent channel flow. *Phys. Fluids* 22:1233–39
Kristoffersen R, Andersson HI. 1993. Direct simulations of low-Reynolds-number turbulent flow in a rotating channel. *J. Fluid Mech.* 256:163–97
Kuo AY-S, Corrsin S. 1971. Experiments on internal intermittency and fine-structure distribution functions in fully turbulent fluid. *J. Fluid Mech.* 50:285–320
Kuroda A. 1990. *Direct numerical simulation of Couette-Poiseuille flows*. EngD thesis, University of Tokyo
Lamb H. 1916. *Hydrodynamics*. Cambridge: University Press
Le H, Moin P. 1994. Direct numerical simulation of turbulent flow over a backward-facing step. *Rep. TF-58*, Thermosci. Div., Dept. Mech. Eng., Stanford Univ., Calif.
Lee C, Kim J, Babcock D, Goodman R. 1997. Application of neural networks to turbulence control for drag reduction. *Phys. Fluids* 9:1740–47
Lee MJ, Kim J, Moin P. 1990. Structure of turbulence at high shear rate. *J. Fluid Mech.* 216:561–83
Lee MJ, Reynolds WC. 1985. Numerical experiments on the structure of homogeneous turbulence. *Rep. TF-24*, Thermosci. Div., Dept. Mech. Eng., Stanford Univ., Calif.
Lee S, Lele SK, Moin P. 1991. Eddy-shocklets in decaying compressible turbulence. *Phys. Fluids A* 3:657–64
Lee S, Lele SK, Moin P. 1992a. Simulation of spatially evolving compressible turbulence and the applicability of Taylor's hypothesis. *Phys. Fluids A* 4:1521–30
Lee S, Lele SK, Moin P. 1993. Direct numerical simulation of isotropic turbulence interact-

ing with a weak shock wave. *J. Fluid Mech.* 251:533–62. Corrigendum in 264:373–74

Lee S, Lele SK, Moin P. 1997. Interaction of isotropic turbulence with shock waves: effect of shock strength. *J. Fluid Mech.* 340:225–47

Lee S, Moin P, Lele SK. 1992b. Interaction of isotropic turbulence with a shock wave. *Rep. TF-52*, Thermosci. Div., Dept. Mech. Eng., Stanford Univ., Calif.

Lele SK. 1992. Compact finite difference schemes with spectral-like resolution. *J. Comp. Phys.* 103:16–42

Lele SK. 1997. Computational aeroacoustics: a review. *AIAA pap. 97–0018*

Lesieur M, Métais O. 1996. New trends in large-eddy simulations of turbulence. *Annu. Rev. Fluid Mech.* 28:45–82

Lumley JL. 1967. The structure of inhomogeneous turbulent flows. In *Atmospheric Turbulence and Radio Wave Propagation*, ed. AM Yaglom, VI Tatarsky, pp. 166–76. Moscow: NAUKA

Lund TS, Wu X, Squires KD. 1996. On the generation of turbulent inflow conditions for boundary layer simulations. In *Annu. Res. Briefs—1996*, pp. 281–95. Center Turbul. Res., Stanford Univ.

Mahesh K, Lee S, Lele SK, Moin P. 1995. The interaction of an isotropic field of acoustic waves with a shock wave. *J. Fluid Mech.* 300:383–407

Mahesh K, Moin P, Lele SK. 1996. The interaction of a shock wave with a turbulent shear flow. *Rep. TF-69*, Thermosci. Div., Dept. Mech. Eng., Stanford Univ., Calif.

Mahesh K, Lele SK, Moin P. 1997. The influence of entropy fluctuations on the interaction of turbulence with a shock wave. *J. Fluid Mech.* 334:353–79

Mansour NN, Kim J, Moin P. 1988. Reynolds-stress and dissipation-rate budgets in a turbulent channel flow. *J. Fluid Mech.* 194:15–44

Marasli B, Champagne FH, Wygnanski I. 1992. Effect of travelling waves on the growth of a turbulent plane wake. *J. Fluid Mech.* 235:511–28

Moin P. 1997. Progress in large eddy simulation of turbulent flows. *AIAA pap. 97–0749*

Moin P, Bewley T. 1995. Application of control theory to turbulence. *Proc. Australas. Fluid Mech. Conf., 12th, Sydney*, p. 109

Moin P, Kim J. 1982. Numerical investigation of turbulent channel flow. *J. Fluid Mech.* 118:341–77

Moin P, Kim J. 1985. The structure of the vorticity field in turbulent region flows. Part 1: Analysis of instantaneous fields and statistical correlations. *J. Fluid Mech.* 200:471–509

Moin P, Moser RD. 1989. Characteristic-eddy decomposition of turbulence in a channel. *J. Fluid Mech.* 155:441–64

Moin P, Spalart PR. 1987. Contributions of numerical simulation databases to the physics, modeling, and measurement of turbulence. *NASA TM 100022*

Moin P, Shih T-H, Driver D, Mansour NN. 1990. Direct numerical simulation of a three-dimensional turbulent boundary layer. *Phys. Fluids A* 2:1846–53

Moser RD, Moin P. 1987. The effects of curvature in wall-bounded turbulent flows. *J. Fluid Mech.* 175:479–510

Moser RD, Rogers MM, Ewing DW. 1997. Self-similarity of time-evolving plane wakes. *J. Fluid Mech.* In press. Also 1994 *NASA TM 108815*

Na Y, Moin P. 1996. Direct numerical simulation of turbulent boundary layers with adverse pressure gradient and separation. *Rep. TF-68*, Thermosci. Div., Dept. Mech. Eng., Stanford Univ., Calif.

Naqwi AA, Reynolds WC. 1987. Dual cylindrical wave laser-doppler method for measurement of skin friction in fluid flow. *Rep. TF-28*, Thermosci. Div., Dept. Mech. Eng., Stanford Univ., Calif.

Neves JC, Moin P, Moser RD. 1994. Effects of convex transverse curvature on wall-bounded turbulence. Part 1. The velocity and vorticity. *J. Fluid Mech.* 272:349–81

Niederschulte MA, Adrian RJ, Hanratty TJ. 1990. Measurement of turbulent flow in a channel at low Reynolds numbers. *Exp. Fluids* 9:222–30

Nishino K, Kasagi N. 1989. Turbulence statistics measurement in a two-dimensional channel flow using a three-dimensional particle tracking velocimeter. *Proc. Symp. Turbul. Shear Flows, 7th, Stanford, pp. 22.1.1–6*, Stanford: CTR

Ohkitani K, Kida S. 1992. Triad interactions in a forced turbulence. *Phys. Fluids A* 4:794–802

Orszag SA, Patterson GS. 1972. Numerical simulation of three-dimensional homogeneous isotropic turbulence. *Phys. Rev. Lett.* 28:76–79

Overholt MR, Pope SB. 1996. Direct numerical simulation of a passive scalar with imposed mean gradient in isotropic turbulence. *Phys. Fluids* 8:3128–48

Parneix S, Durbin PA. 1996. A new methodology for turbulence modelers using DNS database analysis. *Annu. Res. Briefs—1996, pp. 17–30*. Center Turbul. Res., Stanford Univ.

Patterson GS, Orszag SA. 1971. Spectral calculations of isotropic turbulence: efficient removal of aliasing interaction. *Phys. Fluids* 14:2538–41

Perot B, Moin P. 1995a. Shear-free turbulent boundary layers. Part 1. Physical insights

into near-wall turbulence. *J. Fluid Mech.* 295:199–227
Perot B, Moin P. 1995b. Shear-free turbulent boundary layers. Part 2. New concepts for Reynolds stress transport equations modeling of inhomogeneous flows. *J. Fluid Mech.* 295:229–45
Perry AE. 1982. *Hot-Wire Anemometry*. Oxford: Clarendon
Perry AE, Henbest S, Chong MS. 1986. A theoretical and experimental study of wall turbulence. *J. Fluid Mech.* 165:163–99
Pompeo L, Thomann H. 1993. Quadruple hot-wire probes in a simulated wall flow. *Exp. Fluids* 14:145–52
Poinsot TJ, Lele SK. 1992. Boundary conditions for direct simulation of compressible viscous reacting flow. *J. Comp. Phys.* 101:104–29
Pumir A. 1994. A numerical study of the mixing of a passive scalar in three dimensions in the presence of a mean gradient. *Phys. Fluids* 6:2118–32
Rai MM, Moin P. 1991. Direct simulations of turbulent flow using finite-difference schemes. *J. Comp. Phys.* 96:15–33
Rai MM, Gatski TB, Erlebacher G. 1995. Direct simulation of spatially evolving compressible turbulent boundary layers. *AIAA pap. 95–0583*
Reynolds WC. 1976. Computation of turbulent flows. *Annu. Rev. Fluid Mech.* 8:183–208
Riley JJ, Metcalfe RW. 1980. Direct numerical simulation of a perturbed, turbulent mixing layer. *AIAA pap. 80–0274*
Robinson SK. 1991. Coherent motions in the turbulent boundary layer. *Annu. Rev. Fluid Mech.* 23:601–39
Rodi W, Mansour NN. 1993. Low Reynolds number $k - \epsilon$ modeling with the aid of direct simulation data. *J. Fluid Mech.* 250:509–29
Rogallo RS. 1981. Numerical experiments in homogeneous turbulence. *NASA TM-81315*
Rogallo RS, Moin P. 1984. Numerical simulation of turbulent flows. *Annu. Rev. Fluid Mech.* 16:99–137
Rogers MM, Moin P, Reynolds WC. 1986. The structure and modeling of the hydrodynamic and passive scalar fields in homogeneous turbulent shear flow. *Rep. TF-25*, Thermosci. Div., Dept. Mech. Eng., Stanford Univ., Calif.
Rogers MM, Moin P. 1987. The structure of the vorticity field in homogeneous turbulent flows. *J. Fluid Mech.* 176:33–66
Rogers MM, Moser RD. 1994. Direct simulation of a self-similar turbulent mixing layer. *Phys. Fluids A* 6:902–23
Ruetsch GR, Maxey MR. 1991. Small-scale features of vorticity and passive scalar fields in homogeneous isotropic turbulence. *Phys. Fluids A* 3:1587–97
Saddoughi SG, Veeravalli SV. 1994. Local isotropy in turbulent boundary layers at high Reynolds number. *J. Fluid Mech.* 268:333–72
Sarkar S, Erlebacher G, Hussaini MY. 1991. Direct simulation of compressible turbulence in a shear flow. *Theor. Comput. Fluid Dyn.* 2:291–305
Sendstad O, Moin P. 1992. The near wall mechanics of three-dimensional turbulent boundary layers. *Rep. TF-57*, Thermosci. Div., Dept. Mech. Eng., Stanford Univ., Calif.
She Z-S, Jackson E, Orszag SA. 1990. Intermittent vortex structures in homogeneous isotropic turbulence. *Nature* 344:226–28
Sherman FS. 1955. A low-density wind-tunnel study of shock-wave structure and relaxation phenomena in gases. *NASA TN-3298*
Shih T-H. 1996. Developments in computational modeling of turbulent flows. *NASA CP-198458*
Shu C-W, Osher S. 1988. Efficient implementation of essentially non-oscillatory shock-capturing schemes. *J. Comp. Phys.* 77:439–71
Shu C-W, Osher S. 1989. Efficient implementation of essentially non-oscillatory shock-capturing schemes, II. *J. Comp. Phys.* 83:32–78
Siggia ED. 1981. Numerical study of small-scale intermittency in three-dimensional turbulence. *J. Fluid Mech.* 107:375–406
Spalart PR. 1986. Numerical study of sink-flow boundary layers. *J. Fluid Mech.* 172:307–28
Spalart PR. 1988. Direct numerical simulation of a turbulent boundary layer up to $R_\theta = 1410$. *J. Fluid Mech.* 187:61–98
Spalart PR, Moser RD, Rogers MM. 1991. Spectral methods for the Navier-Stokes equations with one infinite and two periodic directions. *J. Comp. Phys.* 96:297–324
Speziale CG. 1991. Analytical methods for the development of Reynolds-stress closures in turbulence. *Annu. Rev. Fluid Mech.* 23:107–57
Speziale CG. 1994. A review of Reynolds stress models for turbulent shear flows. *Proc. Symp. Nav. Hydrodyn., 20th, Santa Barbara, CA.*
Sreenivasan KR, Antonia RA. 1997. The phenomenology of small-scale turbulence. *Annu. Rev. Fluid Mech.* 29:435–72
Sumitani Y, Kasagi N. 1995. Direct numerical simulation of turbulent transport with uniform wall suction and injection. *AIAA J.* 33:1220–28
Suzuki Y, Kasagi N. 1992. Evaluation of hot-wire measurements in wall shear turbulence using a direct numerical simulation database. *Exp. Therm. Fluid Sci.* 5:69–77
Tam CKW. 1995. Computational aeroacoustics: issues and methods. *AIAA pap. 95–0677*
Theodorsen T. 1955. The structure of turbu-

lence. In *50 Jahre Grenzschichtforsung*, ed. H Görtler, W Tollmien, pp. 55–62. Braunschweig: F. Viewig

Thomas NH, Hancock PE. 1977. Grid turbulence near a moving wall. *J. Fluid Mech.* 82:481–96

Thompson PA. 1984. *Compressible Fluid Dynamics*. New York: McGraw-Hill

Townsend AA. 1976. *The Structure of Turbulent Shear Flow*. Cambridge: Cambridge Univ. Press

Uzkan T, Reynolds WC. 1967. A shear-free turbulent boundary layer. *J. Fluid Mech.* 28:803–21

Vincent A, Meneguzzi M. 1991. The spatial structure and statistical properties of homogeneous turbulence. *J. Fluid Mech.* 225:1–20

Vincent A, Meneguzzi M. 1994. The dynamics of vorticity tubes in homogeneous turbulence. *J. Fluid Mech.* 258:245–54

Vreman AW, Sandham ND, Luo KH. 1996. Compressible mixing layer growth rate and turbulence characteristics. *J. Fluid Mech.* 320:235–58

Wallace JM, Foss JF. 1995. The measurement of vorticity in turbulent flows. *Annu. Rev. Fluid Mech.* 27:479–514

Wang L-P, Chen S, Brasseur JG, Wyngaard JC. 1996. Examination of hypotheses in the Kolmogorov refined turbulence theory through high-resolution simulations. Part 1. Velocity field. *J. Fluid Mech.* 309:113–56

Westphal RV, Johnston JP, Eaton JK. 1984. Experimental study of flow reattachment in a single-sided sudden expansion. *Rep. MD-41*, Thermosci. Div., Dept. Mech. Eng., Stanford Univ., Calif.

Weygandt JH, Mehta RD. 1993. Three-dimensional structure of straight and curved plane wakes. *JIAA TR-110*, Dept. Aeron. Astronaut., Stanford Univ.

Wygnanski I, Champagne F, Marasli B. 1986. On the large-scale structures in two-dimensional small-deficit turbulent wakes. *J. Fluid Mech.* 169:31–71

Wyngaard JC. 1969. Spatial resolution of the vorticity meter and other hot-wire arrays. *J. Sci. Instr. (J. Phys. E) Ser. 2* 2:983–87

Xu C, Zhang Z, den Toonder JMJ, Nieuwstadt FTM. 1996. Origin of high kurtosis levels in the viscous sublayer. Direct numerical simulation and experiment. *Phys. Fluids* 8:1938–44

Yeung PK, Girimaji SS, Pope SB. 1990. Straining and scalar dissipation on material surfaces in turbulence: implications for flamelets. *Combust. Flame* 79:340–65

Yeung PK, Brasseur JG. 1991. The response of isotropic turbulence to isotropic and anisotropic forcing at the large scales. *Phys. Fluids A* 3:884–97

Zang TA. 1991. On the rotation and skew-symmetric forms for incompressible flow simulations. *Appl. Num. Math.* 7:27–40

Zeman O. 1990. Dilatation dissipation: the concept and application in modeling compressible mixing layers. *Phys. Fluids A* 2:178–88

Zhou Y. 1993. Interacting scales and energy transfer in isotropic turbulence. *Phys. Fluids A* 5:2511–24